

Improved Numerical Procedures for Soil-Structure Interaction
Including Simulation of Construction Sequences,

by

John Gwin Lightner, III

Thesis submitted to the Graduate Faculty of the
Virginia Polytechnic Institute and State University
in partial fulfillment of the requirements for the degree of
MASTER OF SCIENCE
in
Civil Engineering

APPROVED:

C.S. Desai

D.N. Contractor

R.D. Krebs

A.E. Somers

September, 1979
Blacksburg, Virginia

ACKNOWLEDGEMENTS

I would like to express my deepest appreciation for the support of my wife, Yvette, without whose help this work would never have been accomplished.

Appreciation is extended to Dr. C.S. Desai for his guidance and support. A special thanks goes to Dr. S. Sture for his comments and suggestions.

TABLE OF CONTENTS

ACKNOWLEDGEMENTS	ii
Chapter	page
I. INTRODUCTION	1
motivations and objectives	1
description of various techniques	2
scope of work	3
outline of chapters	4
II. LITERATURE REVIEW	6
introduction	6
basic fem	6
embankments	7
excavations	8
interface elements	10
constitutive models	11
comments	12
III. THEORETICAL DEVELOPMENTS	13
introduction	13
irregular geometries	13
material modeling	15
contact problems (soil-structure interaction)	20
construction sequences	22
comments	29
IV. FORMULATION	30
introduction	30
basic formulation	31
material models	37
linear elastic	37
nonlinear elastic	38
elastic-plastic	39
other element types	46
interface element	46
bar elements	53
construction sequences	56
in situ	56
dewatering	57
excavation	60

	deposition or embankment	62
	tie-backs	64
	structural element placement	66
V.	CODING	67
	introduction	67
	philosophy	67
	features of program	68
	coding difficulties	72
	comments	77
VI.	VERIFICATION OF CODE	78
	Introduction	78
	General Verification	78
	distorted element tests	80
	pure beam bending problem	83
	thick-cylinder problem	86
	hyperbolic test	90
	cap model test	95
	bar element test	98
	interface element test	101
	soil-interface study	104
	Construction Sequences Verification	108
	in situ	110
	dewatering	110
	embankment	110
	excavation	113
	tie-back wall example	113
	advanced problems	120
	footing problem	120
	dam with sequential embankment	122
	retaining wall	126
	Comments	130
VII.	CONCLUSIONS	132
	Summary	132
	Future Recommendations	133
	REFERENCES	134
	VITA	141

LIST OF TABLES

Table	page
1. Comparison of Two and Three Point Integration . . .	81
2. Distorted Element Test Results	85
3. Results for Beam Bending Problem	88
4. Axisymmetric Problem Results	92
5. Material Parameters for Hyperbolic Test	94
6. One-Dimensional Test Results	102
7. Interface Parameters for Soil-Interface Test . . .	106
8. Results of Soil-Interface Test	107
9. Material Properties of Simple Retaining Wall . . .	117
10. Material Properties for Otter Brook Dam	125

LIST OF FIGURES

Figure	page
1. Basic Plane Element	33
2. Interface Element	48
3. Behavior of Interfaces	51
4. Bar Elements	55
5. Example of Dewatering Mesh	59
6. Tie-back Illustration	65
7. Unloading Stress-Strain Response	75
8. Single Test Element Mesh	79
9. Distorted Element Geometry	82
10. Meshes for Distorted Element Tests	84
11. Pure Beam Bending Problem	87
12. Axisymmetric Pressure Vessel	91
13. Hyperbolic Test Problem	93
14. Hyperbolic Test Problem Results	96
15. Cap Model Test Problem	97
16. Cap Model Test Results	99
17. Bar Element Test Problem	100
18. Interface Element Test Problem	103
19. Mesh for Soil Interface Test	105
20. Construction Sequences Debugging Mesh	109
21. One-Dimensional Initial Stress Results	111
22. One-Dimensional Dewatering Results	112

23. One-Dimensional Excavation Results 114

24. Simple Retaining Wall Problem 115

25. Wall Deflection of Simple Retaining Wall 118

26. Surface Settlement Behind Simple Retaining Wall . 119

27. Footing Problem 121

28. Load-Deflection Curve of Footing 123

29. Geometry and Mesh for Otter Brook Dam 124

30. Displacement of Otter Brook Dam Face 127

31. Mesh for Passive Earth Pressure Test 129

32. Results for Passive Earth Resistance Test 131

Chapter I

INTRODUCTION

1.1 MOTIVATIONS AND OBJECTIVES

The advent of the modern digital computer has lead to increased use of numerical models to simulate various physical phenomena. The Finite Element Method (FEM) is one such model which has been used extensively for solving complex engineering problems. Simulation of construction sequences and soil-structure interaction is one such problem to which the FEM has been applied.

Accurate simulation of construction sequences and soil-structure interaction has been attempted many times in the past. Most of these attempts have proven to be successful only for limited classes of construction sequences and soil-structure interaction problems. The difficulty occurs due to factors such as nonlinear materials, complex geometries, contact phenomenon between soil and structure and nonhomogeneous materials. The FEM is capable of handling many of these factors with considerably less effort than other numerical or analytical techniques. The work presented here endeavors to extend and improve, in a unified manner, on formulations and codes developed in the past.

1.2 DESCRIPTION OF VARIOUS TECHNIQUES

The FEM is a numerical technique based on discretization and interpolation. Its advantages are rather great compared to other methods such as the finite difference method. The FEM's major drawback is its generally higher cost in computer time as compared to other methods such as the finite difference method or the boundary integral method. However, as the complexity of the problem increases, the FEM becomes more and more competitive in this respect. The major strong points of the FEM are its ability to account for complex geometries, nonhomogeneities and material nonlinearities.

The basic idea in the FEM is to divide the continuum into discrete subdomains called elements. These elements are connected at discrete points called nodes, which lie on the element boundaries. The form of the solution for each element is assumed a priori by using appropriate interpolation functions for the unknown quantities within an element and from node to node. The solution for the total domain is found by solving the set of simultaneous equations arising from assembling the equations for all of the elements.

There are four main types of finite element formulations based on variational principles (energy methods). They are the displacement approach, the equilibrium approach, the hybrid approach and the mixed approach. Each of these approaches have their own strengths and weaknesses. A displacement approach model was chosen for this research due to its simplicity and the availability of vast amounts of knowledge on it.

1.3 SCOPE OF WORK

Derivation of a formulation for a displacement FEM model for simulation of construction sequences including soil-structure interaction was the major result of this research. The major sequences considered were initial stress state (in situ), consolidation (dewatering), excavation, deposition or embankment, tie-backs and structural components.

The material nonlinearity of the soil was modeled by making several different assumptions such as linear elasticity, nonlinear elasticity and plasticity. A FORTRAN computer code was written to implement the formulation. This program for modeling SEquential CONstruction (SEQCON) represents the bulk of the work. It is intended to be a

practical tool for use by engineers in the construction area.

1.4 OUTLINE OF CHAPTERS

The research consisted of three major sections. These sections are the formulation of the model, the coding of the formulation and the verification of the code.

The formulation of the model is discussed in chapters I through V. Chapter I provides the introduction and discusses the choice of the basic model type. Chapter II contains a literature review and highlights past work in the area of construction sequences and soil-structure interaction. Chapter III discusses the physical nature of the various contributions to the simulation problem including geometry and constitutive modeling. Chapter IV contains the actual derivation of the various parts of the formulation.

The coding of the formulation is explained in chapter V. A great deal of emphasis was spent in obtaining an efficient code which is easy to implement. The details of how this was accomplished are included in this chapter.

Verification of the computer code is one of the more important sections. The verification procedure is outlined and discussed in chapter VI. It is in this chapter that the various capabilities of the code are demonstrated. The importance of this section is due to the need to establish the validity of the program and to build confidence in the mind of the user.

Chapter II

LITERATURE REVIEW

2.1 INTRODUCTION

A review of the past work in the area of finite elements and construction sequences was performed in order to provide a basis for the present research. Emphasis was placed on the review of previous models for simulation of construction sequences. The description of these models generally included such subjects as basic FEM procedures, material models and interface elements. Although this review is not complete, an attempt was made to provide an overview of the history and the state-of-the-art of the simulation of sequential construction.

2.2 BASIC FEM

The FEM has been popular for many years now. Most of the general aspects of the FEM have been described in books. Authors such as Desai and Abel (19), Desai (17), Oden and Reddy (48), Zienkiewicz (57), and others (2) have presented complete details on the basic FEM. Therefore, only topics relevant to sequential construction steps such as embankments and excavations will be discussed in detail.

Most of these specialized topics are only touched upon in the books mentioned above.

2.3 EMBANKMENTS

One of the earlier works on embankments was performed by Goodman and Brown (27). They recognized the error in using direct gravity turn on analysis and devised an incremental solution based on closed form elasticity solutions. Only the stresses and equilibrium of the embankment were analysed.

One of the earlier studies on embankment analysis which considered sequential deformation of the system was by Clough and Woodward (14). Their work considered most factors of simulating embankment construction that are used now. These include incremental solutions and nonlinear material properties. Emphasis was placed on deformations. They contended that although most embankment designs satisfied stability requirements, often excessive deformations could cause problems.

Kulhawy, Duncan and Seed (42) presented the use of the FEM for embankment analysis using a hyperbolic law to simulate stress-strain curves. Their work is an extension of Clough and Woodward's work (14).

2.4 EXCAVATIONS

Finite element modeling of excavations was begun very shortly after the FEM became available. Brown and King (3) did some of the earlier analyses in this area. They extended the work of Goodman and Brown (27) on embankments for application to the simulation of excavation. No retaining structures were considered. They developed a general FEM program for modeling both excavation and embankments. Major emphasis was placed on equilibrium and stability considerations.

Clough and Duncan (9,8) made important advances in modeling excavations. They developed a program based on four node quadrilaterals for simulation of general construction sequences including retaining structures and interface elements. Interpolation of the stresses of several elements was used to calculate the stress on the excavated surface. Use of a nonlinear elastic material model was made. Results of finite element predictions for various assumptions of wall roughness were compared to theoretical solutions and field observations for lock structures.

Design and analysis of a tied-back wall system was done by Clough, Weber and Lamont (13). The work presented demonstrated the power of FEM modeling of excavation and sequential construction in application to design. The FEM results are compared favorably to field measurements.

Desai, Johnson and Hargett (21) applied the FEM with sequential construction to the problem of a gravity lock on pile foundations. The results were compared with field observations. They pointed out various limitations of previous models for simulating construction sequences.

Christian and Wong (6) demonstrated that numerical procedures involving excavation assuming linear elastic material could be in serious error. They showed that excavating a straight cut in one lift was not equal to using several lifts. They reasoned this was due to inability of lower order elements to model the high stress gradients at the toe of the excavation.

The validity of the plane strain assumption for modeling tied-back retaining walls was addressed by Tsui and Clough (56). Through the use of laboratory models, closed form solutions and numerical methods they concluded that the

plane strain assumption can be valid for many conventional tie-back spacings. For walls which use soldier piles with wide spacing the use of plane strain models may be in error.

Clough and Mana (10) demonstrated the usefulness of a linear strain isoparametric quadrilateral for tied-back and braced walls. Their major contribution was a procedure for obtaining an approximate stress free boundary by satisfying total element equilibrium.

One of the most recent advances in FEM model of excavations was made by Osaimi and Clough (49). They developed a model which accounts for excavation, retaining structures and consolidation. The inclusion of a coupled consolidation formulation provides a means of accounting for pore water pressure changes in a consistent manner.

2.5 INTERFACE ELEMENTS

Interface or joint elements have often been used to account for earth-structure interactions. One of the earliest joint elements was developed by Goodman, Taylor and Brekke (29). It was initially developed for modeling rock joints. Desai (18) and others (9,21) have adopted the element for use in soil-structure interaction problems. The

basic features of the Goodman, Taylor and Brekke model are that it is based on relative displacements as quasi strains and assumes zero joint thickness. Although relative displacements are used in the formulation, the element equations contain nodal displacements as unknowns. Zienkiewicz, et al. (58) has made use of solid isoparametric elements to model interface behavior. Ghaboussi, Wilson and Isenberg (26) have criticized the previous interface elements for a variety of reasons. They have developed an element in which the relative displacements themselves are the unknowns to be solved for. Ghaboussi, Wilson and Isenberg claim better numerical stability among other benefits for their element. However, their formulation may not be much different from the previous approaches.

Herrmann (32) has presented interface modeling as the more general case of contact problem modeling. He does not generally use a specific element for interface modeling, instead, he makes use of springs connecting the two materials across an interface.

2.6 CONSTITUTIVE MODELS

Constitutive models for geologic media have developed greatly in recent years. Several excellent overviews of

constitutive modeling are available. One of the best is by Christian and Desai (5). The reader is referred to their work for a complete review.

2.7 COMMENTS

A critique and the state-of-the-art on various aspects of soil-structure interaction is presented in the text by Desai and Christian (20). Detailed considerations on constitutive laws for geologic media are also presented in this book.

Chapter III

THEORETICAL DEVELOPMENTS

3.1 INTRODUCTION

Simulation of construction sequences and soil-structure interaction requires consideration of various physical characteristics of the problem. An accurate simulation model must consider as many of the factors affecting the process as is possible. The complex nature of construction sequences and soil-structure interaction requires that more factors be considered compared to other common problems. The remainder of this chapter discusses these complexities and describes how they are handled in a numerical procedure.

3.2 IRREGULAR GEOMETRIES

Construction sequences and soil-structure interaction problems usually involve complex geometries. An additional complexity that often occurs during simulation of construction sequences is changes in the geometry of the domain. Two examples of these changes are, excavation during which the domain becomes geometrically smaller, and deposition during which the domain increases. Such domains may include arbitrarily shaped slopes and other factors such as right angles and curves.

Most analytical solution techniques utilize some type of idealized geometry. Most geometries encountered in the simulation of construction sequences have no known closed form solution. The finite difference method may be capable of handling certain levels of complex geometries, but special techniques or efforts are often necessary. Two techniques which can handle irregular geometries quite easily are the FEM and the boundary integral method. The boundary integral method has some other difficulties which will be mentioned later.

There are two major reasons for the FEM's ability to model complex geometries easily. First, element shapes can be arbitrary and can be chosen to fit whatever boundaries that are likely to be encountered. Possible element shapes include triangles and quadrilaterals with various orders of curves for the element sides. Second, and most importantly, elements do not have to be the same size or shape. Using only quadrilaterals it is possible to model a circular boundary by dividing the domain into sufficiently small elements.

3.3 MATERIAL MODELING

Geologic media is well known for its great variation in properties and highly nonlinear constitutive behavior. Real problems dealing with geologic media usually have many layers of material with each layer having different properties. The nonhomogeneity of geologic media is one complexity which precludes the easy use of closed form solutions. The FEM is capable of handling the nonhomogeneous nature of geologic media through its ability to include any number of elements with different materials properties. By dividing the domain in such a way that element boundaries coincide with the interfaces of different materials, nonhomogeneous media can be modeled. Finite element formulations can also be derived wherein the material properties vary within an element.

The nonlinear behavior of geologic media provides one of the more difficult problems in the simulation process. The FEM is capable of accounting for the nonlinearity but it requires the use of an incremental and/or iterative solution approach. The main problem in nonlinear geologic media is not the solution procedure itself. Instead it is the representation of the stress-strain relationship of the material in a realistic manner. The stress-strain

relationship is known as the constitutive law or model of the material. Constitutive models are functions of many variables such as the present stress state, the density, the temperature, the strain state, the water content, the stress history and the type of loading. To determine which of these factors are significant, extensive (laboratory) tests must be performed. A constitutive model may then be derived using the laboratory data as the basis.

Three basic material model classes were considered. They are linear elastic, non-linear elastic and elastic-plastic. Each of these model classes are applicable to geologic media although the most realistic models are probably those based on plasticity.

Linear elastic models are the simplest to derive and use. They are also the least accurate since the nonlinear nature of the problem is ignored. Their main use can be for initial studies of simulation problems. For problems with small displacements and stresses, the linear elastic model may provide reasonable results. There are only two material parameters required to completely define the behavior for a linear elastic and isotropic material. Overall, the linear elastic model has limited value in most soil-structure interaction problems including simulation of construction.

Nonlinear elastic models represent the first step toward a true nonlinear constitutive law. These models are based on a piecewise linear elastic assumption and as such are merely an extension of linear elasticity. The procedure followed is to modify the (two) material parameters from linear elasticity in an incremental fashion to follow nonlinear material behavior. The material parameters are often taken to be functions of the current stress state. Several different models have been derived in this class. Their basic feature is that various laboratory test results are represented in either a tabular form or in a direct functional form. Most of the models are assumed to fit some type of function such as a hyperbola, spline, polynomial or exponential. Hyperbolas are the most popular functions in use at this time although others such as splines or modified Ramberg-Osgood may be superior.

Hyperbolic models have been used for several years and there is a great deal of information available of their use. They are relatively easy to implement and to use in solving general simulation problems in construction sequences. Their major drawback is the inconsistency of their formulation. They can be used to represent only one set of stress-strain curves at a time. Hence, they cannot be used

for problems involving large variations of stress paths. Therefore their use in soil-structure interaction problems is limited and great caution is needed when they are used.

Plasticity models can allow consideration of stress history and stress paths. Two plasticity models which will be used here are a Drucker-Prager type model and a cap type model. Most plasticity models are based on stress invariants. They are usually derived in a consistent fashion and can lead to well behaved models for a given class of problems. Most simple plasticity models do not adequately represent geologic media and it is necessary to use more sophisticated types.

Plasticity models make use of so called yield surfaces for determination of the state of the body. At any point in a body either the medium is on the yield surface or below it. The body is said to be plastic if the state of stress is on the yield surface and elastic if below it. The yield surface can be either some type of failure envelope or a pre-failure yield envelope. Yield surfaces are usually direct functions of the stress invariants and often some additional quantity representing the history of loading of the body. The maximum past hydrostatic pressure is one

variable which may be used to represent the history of loading.

The Drucker-Prager model represents one of the simplest models which have been applied to geologic media. They make use of only one yield surface which is defined by (5):

$$f = \sqrt{J_2'} + \alpha I_1 - k = 0 \quad \text{Eq. 3.1}$$

Where

$$J_2' = [(\sigma_{xx} - \sigma_{yy})^2 + (\sigma_{yy} - \sigma_{zz})^2 + (\sigma_{xx} - \sigma_{zz})^2] / 6 \\ + \sigma_{xy}^2 + \sigma_{xz}^2 + \sigma_{yx}^2$$

$$I_1 = \sigma_{xx} + \sigma_{yy} + \sigma_{zz}$$

α, k = material constants

σ_{ij} = stress tensor

Linear elasticity is usually assumed for stress states below the yield surface. The major objection to the Drucker-Prager model is the large volumetric plastic strains which the model predicts. These strains have not been observed in laboratory tests. Therefore the Drucker-Prager model may not be very satisfactory for representing many

geologic materials. It is included here due to its simplicity and as a demonstration of the use of a plasticity model.

Capped yield models represent one of the improved constitutive laws for application to geologic media. Through the use of two or more yield surfaces it is possible to have a continuous nonlinear response. One or more yield surfaces represent the failure envelope in a cap model while the other yield surface allows plastic strains to develop below failure stress states. This pre-failure yield surface is commonly referred to as a cap. The cap is allowed to move depending upon some variable such as the plastic volumetric strain. There are a variety of functions used to describe the cap and failure surfaces. The failure surface is often assumed to be of the Drucker-Prager type while a bullet or ellipse is assumed for the cap.

3.4 CONTACT PROBLEMS (SOIL-STRUCTURE INTERACTION)

Transitions from geologic media to man made structures usually involves large changes in material properties. The changes are often so great that the medium may become discontinuous at the soil-structure interface. The resulting phenomenon, known as soil-structure interaction,

is the most complex factor to be considered in simulating construction sequences. Basically the reason for the difficulty lies in the fact that under compression the interface remains continuous. Tension causes the interface to separate and the body becomes discontinuous. The problem is magnified by the requirement that under compression the interface has infinite normal stiffness while under tension it has zero stiffness. Relative shear movements between the two materials must also be accounted for. For soil-structure interaction problems, shearing behaviour is the important mode to be modeled. Shear strains can be as large as several hundred to several thousand percent at an interface.

Most interface models use the concept of relative displacements to avoid the problem of finite strains. These models use stresses and displacements as basic quantities. They have material parameters which relate the stresses directly to the relative movement of the two materials. These interface models have had limited success for a variety of problems. Often they cause numerical instabilities in a problem. The reason may lie in the inconsistency of their formulation as compared to the two-dimensional solid elements used. Research in this area

is continually going on and hopefully improved interface models will become available in the near future.

3.5 CONSTRUCTION SEQUENCES

The actual steps of construction need to be considered for an accurate simulation. Since the problem is generally nonlinear, the order and manner of the actual construction needs to be taken into account. The problem is to identify the steps in the actual field construction and then reduce them to valid numerical equations. The reduction to the numerical equations needs to include as many of the field conditions as can be thought of. During the formulation of the model is where most simplifying assumptions should occur.

Six main features of construction are considered and a list is given below.

1. in situ - Calculation of the initial stress state of the medium.
2. Dewatering - Process of lowering the initial water table.

3. Excavation - Process of removing material from the domain.
4. Deposition - Process of adding material to the domain.
5. Support system - Procedure of adding bracing, anchors, tie-backs
6. Structure - Process of adding various man made structural components such as concrete and steel to the domain.

The initial stress state in a domain is generally assumed to be known before the solution begins. Obtaining this data is an important and difficult problem.

The procedure to calculate the in situ stresses requires the knowledge of the geometry of the body, the density of the material and the coefficient of lateral earth pressure at rest (45,1). The governing equations are of the following form (40):

$$\sigma_v = \int_0^H \gamma dh \quad \text{Eq. 3.2}$$

$$\sigma_h = K_o \sigma_v \quad \text{Eq. 3.3}$$

Where

σ_v = vertical stress

σ_h = horizontal stress

γ = effective unit weight

H = depth from ground surface

K_o = coefficient of lateral earth
pressure at rest

The process of dewatering is commonly encountered during construction. Usually it is a preliminary step to excavation. The problem occurs when the water table lies above the level of excavation. Dewatering is usually accomplished by installing well points at various places in the domain and then pumping water from the well points. The dewatering causes consolidation process and should be modeled as such.

There are many consolidation models available, each making different assumptions about the nature of the problem. The most sophisticated model is probably Biot's theory of consolidation. Biot's theory is a coupled model

in which deformations of the soil skeleton are linked to the changes in excess pore water pressure. The equations describing Biot's theory of consolidation are:

$$C_{ijkl}\epsilon_{kl,j} + \alpha\delta_{ij}U_{e,j} + X_i = 0 \quad \text{Eq. 3.4}$$

$$\dot{\epsilon}_{kk} + \frac{K_{ij}}{\gamma_w}(U_{,ji} + f_{j,i}) = 0 \quad \text{Eq. 3.5}$$

Where

C_{ijkl} = constitutive matrix of soil skeleton

ϵ_{kl} = strain tensor of soil skeleton

α = interaction coefficient

δ_{ij} = Kronecker delta function

U_e = excess pore pressure

X_i = body force of soil

$\dot{}$ = time drivative of

K_{ij} = Darcy permeability tensor

γ_w = unit weight of fluid

f_j = fluid body force

Excavation is the basic construction process required in most construction jobs. It is used to prepare the foundation of almost all buildings. The simulation of

excavation has great importance due to the large number of buildings constructed in close proximity to existing buildings. The major questions to be answered are what effect will the excavation have on existing buildings and how much bracing will be required to support the excavation. These two questions are quite closely related. The answers to these questions will determine to a great extent the cost of the excavation and foundation.

The physical process of excavation is not very complex and its governing equation is quite basic. Note that while the process itself is simple the actual numerical modeling is not. The difficulties of modeling excavation will be discussed in chapter IV. The governing equation is a statement of the satisfaction of equilibrium at all stages of excavation. The equations are as follows:

$$\sigma_{ij,j} + f_i = 0 \quad \text{Eq. 3.6}$$

Where

σ_{ij} = stress tensor

f_i = body force per unit volume

From the use of equation 3.6 equivalent loads may be found resulting from removal of material from the domain. These loads are then treated like any other surface tractions and the new displacement and stress state may be calculated.

Deposition usually occurs when embankments for buildings, roads and dams are constructed. The procedure in the field usually proceeds in the following manner. Initially a layer of material is deposited evenly over the site of the proposed embankment. The layer is then compacted to some predetermined density to form a section of the embankment. The total embankment is constructed by a series of similar layers or lifts. The material has little strength until the compaction step is performed. Therefore when a lift is placed its main effect is to add a surface loading or traction to the layers beneath it.

The governing equation for deposition is very simple and the problem itself is often well behaved. The monotonic nature of the problem is the main reason that the solution

is comparatively easy. The equation is as follows:

$$F = \int_{V_1} \gamma dV_1 \quad \text{Eq. 3.7}$$

Where

γ = effective unit weight of lift

V_1 = volume of lift

F = surface traction due to lift

Installation of support systems can be considered similar to the prestressing of concrete beams. For example, tie-backs act to prevent tension in the geologic media by imposing an overall compressive stress. The compressive stress is greater than any tension stresses which might result and thereby the soil is always kept in a compressive state. The installation of tie-backs in the field involves three basic steps. The first step is to drill a hole (at an angle to the horizontal) into the face of the excavation. The hole is bored to depth beyond the zone of influence of the excavation. The next step is the installation of the tie-back into the borehole. Installation is accomplished by sliding the tie-back into the hole and then pressure grouting the end of the tie-back to form the anchor. The

tie-back itself usually consists of either steel cables or steel reinforcing rods. Only the last portion of the tie-back is grouted. The remainder of the tie-back is usually encased in a plastic sheath to prevent any transfer of load to the media near the excavation face. The last step is the tensioning of the tie-back to provide the overall compressive stress.

The last feature of a model to simulate construction sequences is the ability to handle the addition of various structural components to the domain. The main requirement is that the structural elements be added or deleted to the domain at the proper stage of construction. The structural elements considered here are generally either retaining walls or tunnel linings.

3.6 COMMENTS

A description of the physical nature and the theory of the simulation of construction sequences has been presented. The details from this description will be used to formulate the simulation model in Chapter IV.

Chapter IV

FORMULATION

4.1 INTRODUCTION

Formulating a model for simulating construction sequences requires considerable judgement. Each facet of the actual process must be accounted for or a reason given for ignoring it. Formulation involves a balancing of accuracy versus cost. More complex formulations are usually more accurate but they are also more expensive. During each step in the formulation it is necessary to ask what is the simplest formulation which will give adequate results. Acknowledgement of the limitations and probable errors must be detailed in the formulation.

Formulation of the sequential construction model was developed in four parts. The basic FEM model is the first part and all of the remaining parts are linked in some manner to it. Modeling of material properties is the second part considered. Development of various special finite elements used forms the third part. The formulation of the various construction sequences is developed last.

4.2 BASIC FORMULATION

Displacement finite element models have been used for a wide range of solid mechanics problems. Their numerical stability and ease of formulation has been demonstrated for many problems. Due to their wide usage, a large amount of information on them is available.

An eight node isoparametric element with quadratic variation of displacements leads to linear stress distributions within the element. The process of construction sequences can involve high stress gradients and therefore the linear stress element was chosen as a compromise between lower and higher order models. Lower order models would not be capable of accurately reflecting the high stress gradients unless a fine mesh was used. Higher order models could be too expensive in terms of computer time. Another difficulty with higher order elements is the requirement in sequential construction problems of a minimum number of elements. A minimum number of elements is required to accurately model the geometry and different materials in the problem. Thus, the increased capability of the high order element would often be under utilized.

Factors considered in the formulation of the element include internal body forces, surface tractions and concentrated loads. The body force is assumed to be only due to gravity and acts in the global Y direction. The surface tractions may vary linearly along the element boundary. Concentrated or point loads may be specified at any nodal point. The quadratic isoparametric formulation allows the element sides to be a parabolic curve. Curved boundaries may be modeled using fewer elements as compared to straight sided linear elements.

An outline of the element formulation will now be given. The basic element used appears in Figure 1. The displacements within the element are assumed to be quadratic functions of the global coordinates. They are expressed as:

$$U(X,Y) = \alpha_1 + \alpha_2 X + \alpha_3 Y + \alpha_4 X^2 + \alpha_5 XY + \alpha_6 Y^2$$

Eq. 4.1

$$V(X,Y) = \beta_1 + \beta_2 X + \beta_3 Y + \beta_4 X^2 + \beta_5 XY + \beta_6 Y^2$$

Eq. 4.2

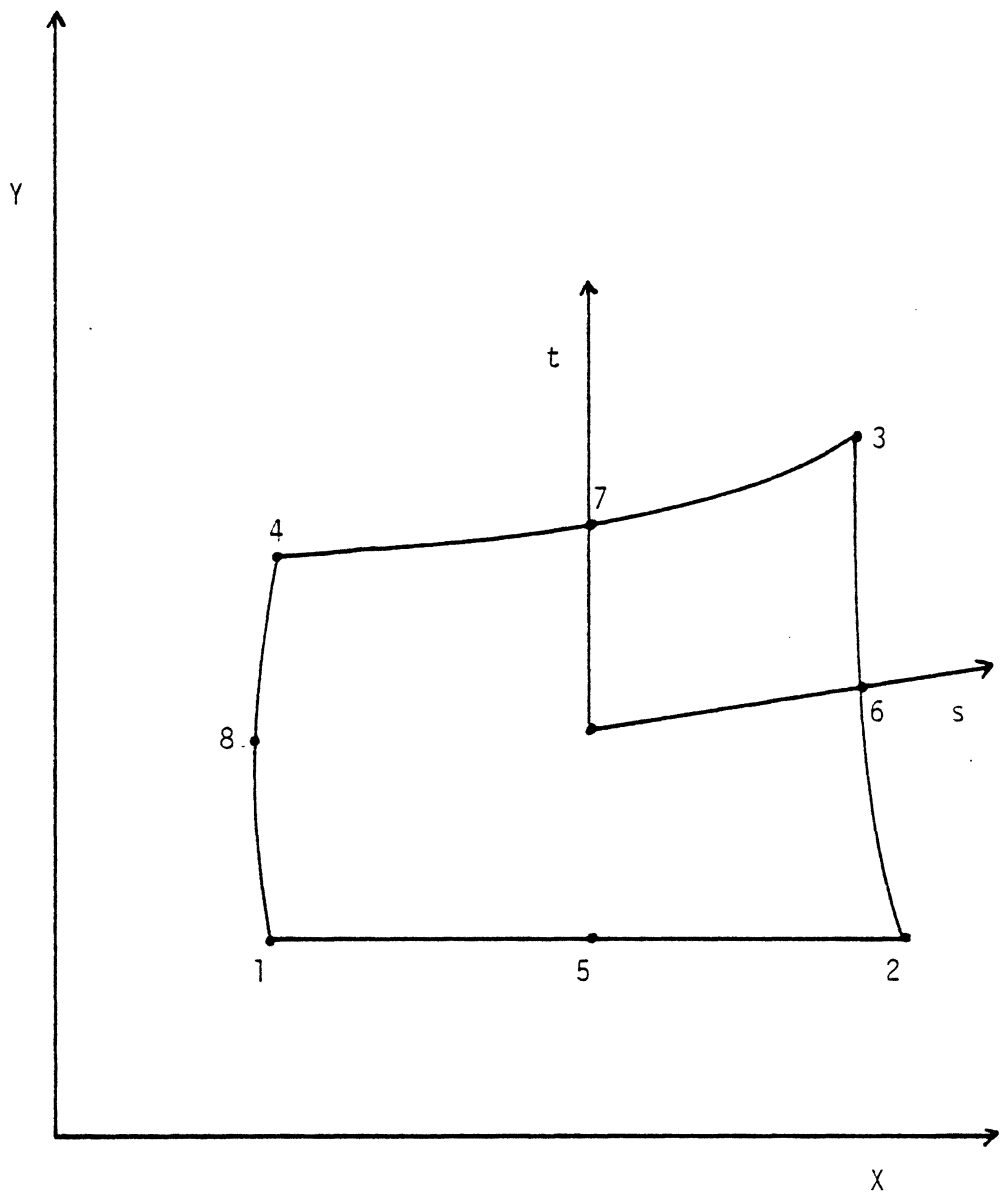


Figure 1: Basic Plane Element

The problem is simplified by making use of a set of local coordinates for the element in which there is a one to one correspondence between local and global coordinates. Using interpolation functions based on local coordinates, the location of any point in the body may be found by interpolation. The following relationship is used:

$$X = \sum_{i=1}^8 N_i X_i \quad \text{Eq. 4.3}$$

$$Y = \sum_{i=1}^8 N_i Y_i \quad \text{Eq. 4.4}$$

Where N_i are defined as the interpolation functions

$$N_i = 1/4(1+ss_i)(1+tt_i)(ss_i+tt_i-1)$$

X, Y = Global coordinates

X_i, Y_i = Global coordinates at node i

s, t = Local coordinates
corresponding to X, Y

s_i, t_i = Local nodal coordinates
corresponding to X_i, Y_i

An isoparametric formulation implies the same approximation for displacements as for the geometry.

Therefore the global displacements are defined as follows:

$$U(s,t) = \sum_{i=1}^8 N_i U_i \quad \text{Eq. 4.5}$$

$$V(s,t) = \sum_{i=1}^8 N_i V_i \quad \text{Eq. 4.6}$$

Where

U, V = Global displacements in X and Y directions respectively

U_i, V_i = Global displacements in X and Y directions respectively at node i

N_i = Same as above

The strains in the element are given by the following equation:

$$\{\epsilon\} = [B]\{q\} \quad \text{Eq. 4.7}$$

Where

$\{\epsilon\}$ = vector of strains

$\{q\}$ = nodal displacements of the element

$[B]$ = transformation matrix for displacement to strain

The displacement approach is based on the principle of minimum potential energy. The functional used is expressed as:

$$\begin{aligned} \pi = & \int_V (1/2 \{\epsilon\}^T [C] \{\epsilon\} - \{v\}^T \{\bar{Y}\}) dV \\ & - \int_{s_1} (\{u\}^T \{\bar{T}_x\} + \{v\}^T \{\bar{T}_y\}) ds_1 \end{aligned} \quad \text{Eq. 4.8}$$

Where

$\{\epsilon\}$ = vector of strains

$[C]$ = constitutive relation between stress and strain

\bar{Y} = body force due to gravity

$\{u\}, \{v\}$ = global displacements

$[\bar{T}_x], [\bar{T}_y]$ = prescribed surface tractions in X and Y directions

s_1 = area over which the surface tractions are specified

After substituting for the various terms, taking variation and equating to zero the following equation results:

$$\begin{aligned} & \int_V ([B]^T [C] [B] \{q\} - [N]^T \{\bar{Y}\}) dV \\ & - \int_{s_1} ([N]^T \{\bar{T}_x\} + [N]^T \{\bar{T}_y\}) ds_1 = 0 \end{aligned} \quad \text{Eq. 4.9}$$

Equation 4.9 is the basic governing equation for a single element based on the displacement approach. Note that only the displacements at the nodes are unknown. Stresses may be calculated by first finding the strains and then using the constitutive matrix as follows:

$$\{\sigma\} = [C][B]\{q\} \quad \text{Eq. 4.10}$$

4.3 MATERIAL MODELS

Four constitutive models to approximate soil or rock behavior were formulated. They range from the simplest possible linear elastic model to a sophisticated cap model.

4.3.1 linear elastic

A linear elastic model was first formulated. The material was assumed to be linear, elastic, and isotropic. These assumptions lead to a constitutive matrix with only two constants, Young's Modulus and Poisson's Ratio. No further discussion of the linear model is needed due to its common usage and simplicity.

4.3.2 nonlinear elastic

Nonlinear elastic models in which the elastic parameters vary in some fashion provide the next step toward a more realistic model. Young's modulus and Poisson's ratio are assumed to be of a nonlinear form. The values of the parameters are as functions of the stress state in the body. The tangent Young's modulus and the tangent Poisson's ratio are assumed to be hyperbolic functions of the stress state in the present model. The equations used for the tangent Young's modulus and the tangent Poisson's ratio are as follows (5,18,42):

$$E_t = \left[1 - \frac{R_f(1 - \sin\phi)(\sigma_1 - \sigma_3)}{2c \cos\phi + 2\sigma_3 \sin\phi} \right]^2 K p_a (\sigma_3/p_a)^n$$

Eq. 4.11

$$\nu_t = \frac{G - F \log(\sigma_3/p_a)}{\left[1 - \frac{(\sigma_1 - \sigma_3)d}{\left[1 - \frac{R_f(\sigma_1 - \sigma_3)(1 - \sin\phi)}{2c \cos\phi + 2\sigma_3 \sin\phi} \right] K p_a (\sigma_3/p_a)^n} \right]^2}$$

Eq. 4.12

where

σ_1, σ_3 = principle stresses

R_f = failure ratio

ϕ, c = Mohr-Coloumb strength parameters

p_a = atmospheric pressure

K, n, G, F, d = experimentally determined
material parameters

Detailed derivations of the hyperbolic formulation are available in (24).

4.3.3 elastic-plastic

Plasticity offers another method of modeling geologic media. It provides a more consistent formulation than the piecewise linear model above. The Drucker-Prager model is one of the simpler plasticity models. Although it is not applicable to soils in general, it is capable of representing some soils. The Drucker-Prager model is based on the extended Mohr-Coulomb failure criteria given by (5,23):

$$S = c + \sigma_n \tan \phi \quad \text{Eq. 4.13}$$

Where

S = Shear strength of media

c = cohesion

σ_n = normal stress

ϕ = internal angle of friction

The yield surface, which is, in this case, a failure surface is defined on the basis of the first and second stress invariants.

$$f = \alpha I_1 + \sqrt{J_2'} - k = 0 \quad \text{Eq. 4.14}$$

Where

α, k = material parameters

An associated flow rule is used which is defined as follows:

$$d\epsilon_{ij}^p = \lambda \frac{\partial f}{\partial \sigma_{ij}} \quad \text{Eq. 4.15}$$

Also

$$d\varepsilon_{ij}^e = d\varepsilon_{ij}^e + d\varepsilon_{ij}^p \quad \text{Eq. 4.16}$$

$$d\sigma_{ij} = C_{ijkl} d\varepsilon_{kl}^e \quad \text{Eq. 4.17}$$

Differentiating equation 4.14, and using equations 4.15, 4.16 and 4.17 to eliminate λ , the following equation results:

$$\begin{aligned} \frac{d\sigma_{ij}}{2G} = d\varepsilon_{ij} - [A(\sigma_{kl}\delta_{ij} + \sigma_{ij}\delta_{kl}) \\ + B\delta_{kl}\delta_{ij} + C\sigma_{ij}\sigma_{kl}]d\varepsilon_{kl} \end{aligned} \quad \text{Eq. 4.18}$$

Where

$$A = \frac{h}{pk}$$

$$B = \left(\alpha - \frac{I_1}{6\sqrt{J_2'}}\right) \frac{p-1}{3ap} - \frac{3Kv}{Ep}$$

$$C = \frac{1}{2kp\sqrt{J_2'}}$$

$$P = \frac{\sqrt{J_2'}}{k} \left(1 + \frac{9\alpha^2 K}{G}\right)$$

$$h = \frac{3K}{2G} \alpha - \frac{I_1}{6\sqrt{J_2'}}$$

K = bulk modulus

E = elastic modulus

ν = Poisson's ratio

G = Shear modulus

For plane strain conditions equation 4.18 reduces to:

$$\begin{aligned} \frac{d\sigma_{11}}{2G} = & (1 - 2A\sigma_{11} - B - C\sigma_{11}^2) d\epsilon_{11} \\ & + [-A(\sigma_{11} + \sigma_{22}) - B - C\sigma_{11}\sigma_{22}] d\epsilon_{22} \\ & + (-A\sigma_{12} - C\sigma_{11}\sigma_{12}) d\gamma_{12} \end{aligned}$$

Eq. 4.19

$$\begin{aligned} \frac{d\sigma_{22}}{2G} = & [-A(\sigma_{11} + \sigma_{22}) - B - C\sigma_{11}\sigma_{22}] d\epsilon_{11} \\ & + (1 - 2A\sigma_{22} - B - C\sigma_{22}^2) d\epsilon_{22} \\ & + (-A\sigma_{12} - C\sigma_{12}\sigma_{22}) d\gamma_{12} \end{aligned}$$

Eq. 4.20

$$\begin{aligned}\frac{d\sigma_{33}}{2G} = & [-A(\sigma_{11} + \sigma_{33}) - B - C\sigma_{11}\sigma_{33}]d\varepsilon_{11} \\ & + [-A(\sigma_{22} + \sigma_{33}) - B - C\sigma_{22}\sigma_{33}]d\varepsilon_{22} \\ & + (-A\sigma_{12} - C\sigma_{12}\sigma_{33})d\gamma_{12}\end{aligned}$$

Eq. 4.21

$$\begin{aligned}\frac{d\sigma_{12}}{2G} = & (-A\sigma_{12} - C\sigma_{11}\sigma_{12})d\varepsilon_{11} \\ & + (-A\sigma_{12} - C\sigma_{12}\sigma_{22})d\varepsilon_{22} \\ & + (\frac{1}{2} - C\sigma_{12}^2)d\gamma_{12}\end{aligned}$$

Eq. 4.22

A, B and C are defined as above.

α and k are defined in terms of the Mohr-Coulomb strength parameters c , the cohesion, and ϕ , the friction angle. For plane strain one relationship between these parameters is the following:

$$\alpha = \frac{\tan\phi}{\sqrt{(9 + 12 \tan^2\phi)}} \quad \text{Eq. 4.23}$$

$$k = \frac{3c}{\sqrt{(9 + 12 \tan^2 \phi)}} \quad \text{Eq. 4.24}$$

For more explicit derivations of the equations above see (5,58).

More advanced plasticity models may be derived by the use of an additional yield surface called a cap. This cap permits plastic flow below the failure surface and can model many more materials than the Drucker-Prager model. The cap model presented here arises from the work presented by Sandler and Rubin (52). In this model an exponential failure surface is used in conjunction with an elliptical cap.

The function for the failure surface is as follows:

$$f_f(J_1) = A - C e^{BJ_1} = \sqrt{J_2'} \quad \text{Eq. 4.25}$$

and for the cap:

$$f_c(J_1, \kappa) = \frac{1}{R} \sqrt{\{[X(\kappa) - L(\kappa)]^2 - [J_1 - L(\kappa)]^2\}} = \sqrt{J_2'} \quad \text{Eq. 4.26}$$

in which:

$$X(\kappa) = \kappa - R f_f(\kappa) \quad \text{Eq. 4.27}$$

$$L(\kappa) = \begin{cases} \kappa & \text{if } \kappa < 0 \\ 0 & \text{if } \kappa \geq 0 \end{cases} \quad \text{Eq. 4.28}$$

The hardening parameter is related to the plastic volumetric strain by the following equations:

$$\bar{\epsilon}_v^p = W[e^{DX(\kappa)} - 1] \quad \text{Eq. 4.29}$$

$$d\bar{\epsilon}_v^p = \begin{cases} d\epsilon_v^p & \text{if } d\epsilon_v^p \leq 0, \text{ or } \kappa < J_1 \text{ and } \kappa < 0 \\ 0 & \text{otherwise} \end{cases} \quad \text{Eq. 4.30}$$

Where

κ = hardening parameter for cap

ϵ_v^p = plastic volumetric strain

A, B, C, D, R, W = material parameters

4.4 OTHER ELEMENT TYPES

The complex nature of simulation of construction sequences requires the use of several one dimensional elements. Three such elements are formulated here. They include an interface element, a linear displacement bar element and a quadratic displacement bar element.

4.4.1 interface element

The interface element used to model the discontinuity between geologic media and man made media is based on the model proposed by Goodman, Taylor and Brekke (29) and later modified and used by Desai (15,18,21). The original element was developed for rock joints, but with the use of proper material parameters it can be applied to soil-structure interfaces.

The basic assumptions involved are that displacements vary linearly along the element and that rotations are not

explicitly considered. The concept of relative displacements are used and they are defined as follows:

$$\begin{Bmatrix} \Delta u_o \\ \Delta v_o \end{Bmatrix} = \frac{1}{2} \begin{bmatrix} -A & 0 & -B & 0 & B & 0 & A & 0 \\ 0 & -A & 0 & -B & 0 & B & 0 & A \end{bmatrix} \begin{Bmatrix} u_1 \\ v_1 \\ u_2 \\ v_2 \\ u_3 \\ v_3 \\ u_4 \\ v_4 \end{Bmatrix} \quad \text{Eq. 4.31}$$

Where

Δu_o = relative displacement or strain
in X direction

Δv_o = relative displacement or strain
in Y direction

$$A = 1 - 2L/\ell$$

$$B = 1 + 2L/\ell$$

u_i, v_i = displacements in X and Y directions
respectively at node i

Now relating the shear and normal stresses to the relative displacements by a stiffness matrix leads to the

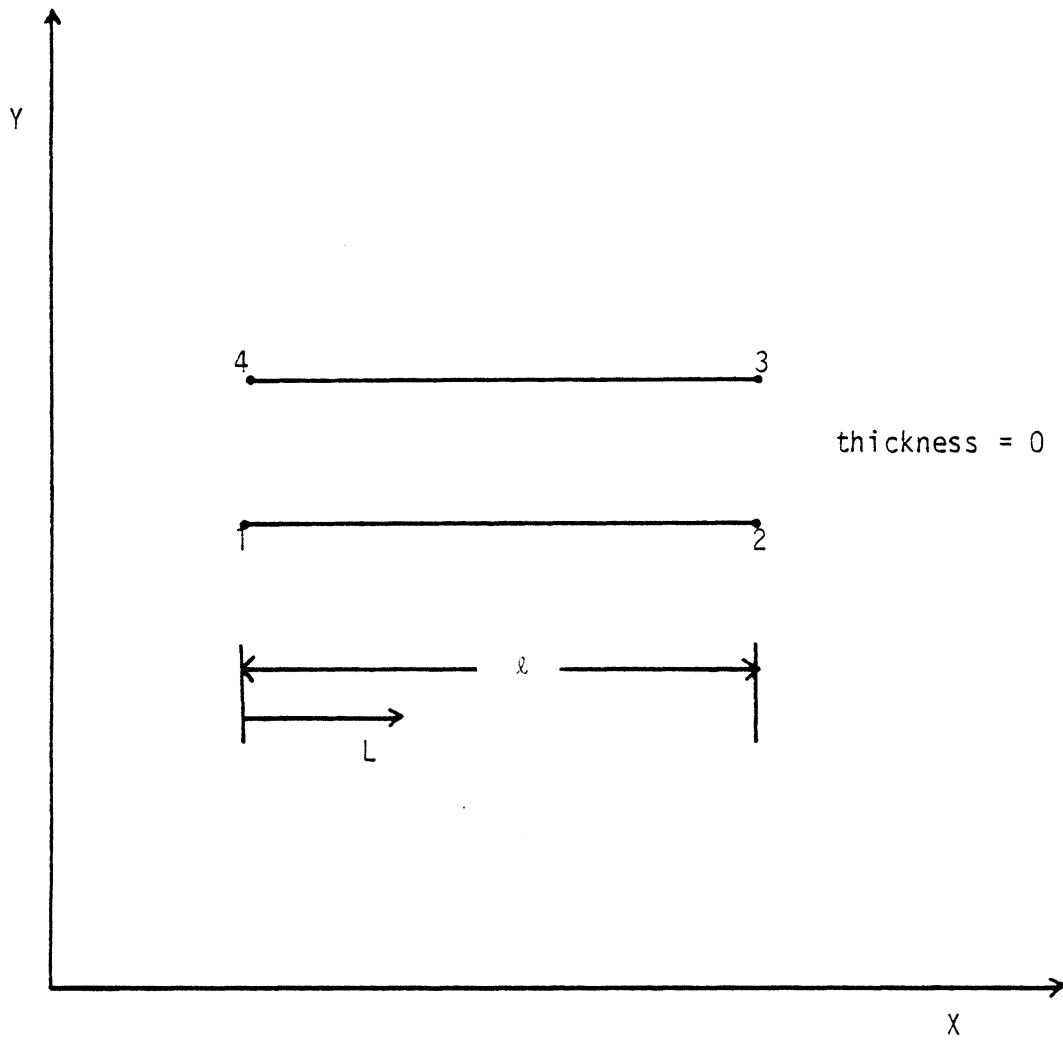


Figure 2: Interface Element

equation:

$$\begin{Bmatrix} \tau \\ \sigma_n \end{Bmatrix} = \begin{bmatrix} K_{ss} & K_{sn} \\ K_{sn} & K_{nn} \end{bmatrix} \begin{Bmatrix} \Delta u_o \\ \Delta v_o \end{Bmatrix} \quad \text{Eq. 4.32}$$

The K_{sn} term is usually taken to be zero due to experimental difficulty in determining its proper value. Using equations 4.31 and 4.32 the local element stiffness matrix is as follows:

$$[K] = \frac{\ell}{6} \begin{bmatrix} 2K_s & 0 & K_s & 0 & -K_s & 0 & -2K_s & 0 \\ & 2K_n & 0 & K_n & 0 & -K_n & 0 & -2K_n \\ & & 2K_s & 0 & -2K_s & 0 & K_s & 0 \\ & & & 2K_n & 0 & -2K_n & 0 & -K_n \\ & & & & 2K_s & 0 & K_s & 0 \\ & & & & & 2K_n & 0 & K_n \\ & & & & & & 2K_s & 0 \\ & & & & & & & 2K_n \end{bmatrix}$$

symmetric

Eq. 4.33

The material parameters of the interface element may either be constants or variables. Two models for material

behavior of interfaces were formulated. The first model was an assumption of linear elasticity of the joint. The effect of this assumption turns out to be that and are bilinear. When the interface is compressed, the shear stiffness will be some constant taken from a laboratory test. The normal stiffness will be taken as a relatively large value to prevent the element from closing to a negative thickness. If the element is under tension, both the shear stiffness and normal stiffness will be set to a relatively small value. This is done to model the gap between soil and structure since in most cases soils cannot maintain tension. No provision for the failure of the interface in compression was made for this model. The next model formulated accounts for most of the phenomenon of interfaces.

A hyperbolic function was used to provide a nonlinear model for the interface element. The basic criterion for failure of the interface in shear is the Mohr-Coloumb criterion (15,18,21):

$$S = C_a + \sigma_n \tan \delta \quad \text{Eq. 4.34}$$

Where

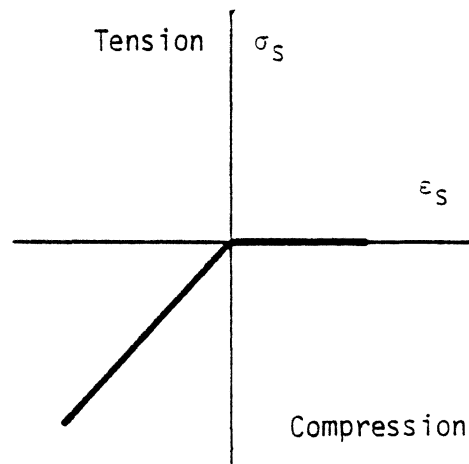
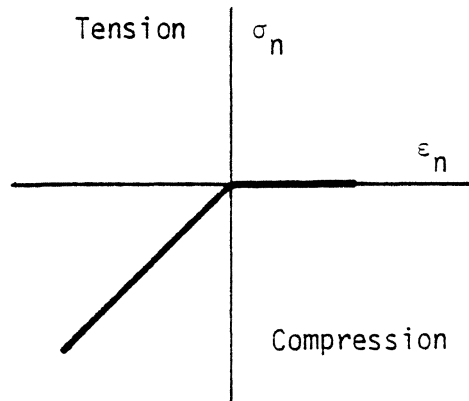


Figure 3: Behavior of Interfaces

C_a = adhesion of soil to structure

δ = friction angle between soil
and structure

The nonlinear behavior up to and including the failure criteria is represented by the following equation:

$$K_{st} = K_j \gamma_w (\sigma_n / p_a)^2 \left[1 - \frac{R_f |\sigma_s|}{C_a + \sigma_n \tan \delta} \right]^2 \quad \text{Eq. 4.35}$$

Where

K_{st} = tangential shear stiffness

K_j = shear stiffness factor

γ_w = unit weight of water

p_a = atmospheric pressure

R_f = failure ratio

C_a, δ = defined as above

Equation 4.35 is valid only for compressive normal stresses. If the normal stress goes into tension the shear stiffness is given a relatively small value. The normal stiffness is defined in the same manner as in the first model.

4.4.2 bar elements

Two bar elements were formulated for use in modeling tie-backs. A quadratric model was derived to provide compatibility between the soil elements and bar elements. A linear model provides a bar element which can be independent of the soil elements.

The linear bar element follows Desai's (17) derivations and the local stiffness matrix is as follows:

$$[K] = \frac{AE}{\ell} \begin{bmatrix} 1 & -1 \\ -1 & 1 \end{bmatrix} \quad \text{Eq. 4.36}$$

Where

A = Area of bar

E = elastic modulus

ℓ = length of the element

The global stiffness of the linear element is as follows:

$$[K] = \frac{AE}{\ell} \begin{bmatrix} C^2 & CS & -C^2 & -CS \\ S^2 & -CS & -S^2 & CS \\ C^2 & CS & S^2 & -CS \\ S^2 & -CS & -S^2 & CS \end{bmatrix} \quad \text{Eq. 4.37}$$

Where

$$C = \cos \alpha$$

$$S = \sin \alpha$$

α = inclination of element with respect to the X axis

The quadratic bar element's local and global stiffness are similar to the linear stiffnesses:

$$[K] = \frac{AE}{3\ell} \begin{bmatrix} 7 & -8 & 1 \\ -8 & 16 & -8 \\ 1 & -8 & 7 \end{bmatrix} \quad \text{Eq. 4.38}$$

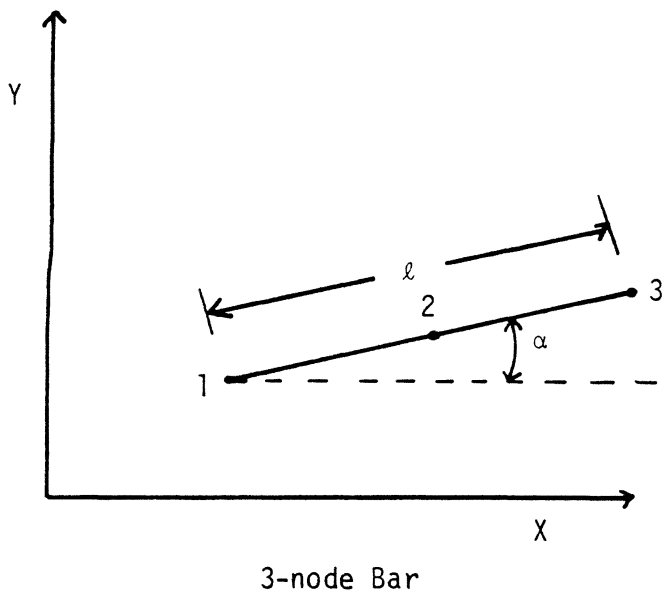
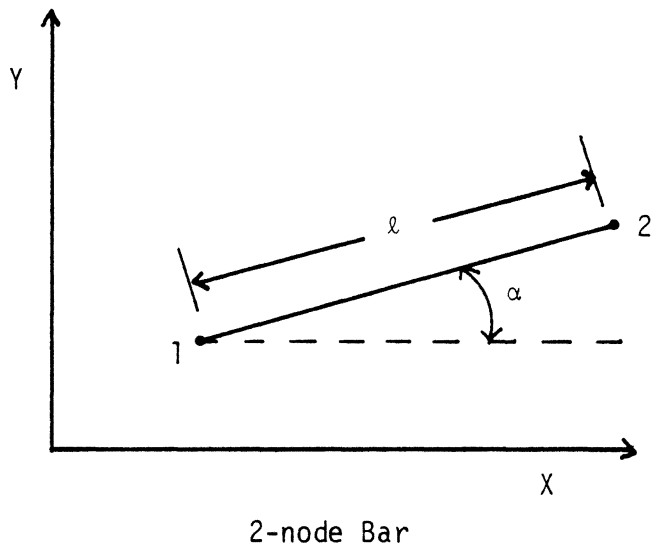


Figure 4: Bar Elements

$$[K] = \frac{AE}{3\ell} \begin{bmatrix} 7C^2 & 7CS & -8C^2 & -8CS & C^2 & CS \\ & 7S^2 & -8CS & -8S^2 & CS & S^2 \\ & & 16C^2 & 16CS & -8C^2 & -8CS \\ & & & 16S^2 & -8CS & -8S^2 \\ \text{symmetric} & & & & 7C^2 & 7CS \\ & & & & & 7S^2 \end{bmatrix}$$

Eq. 4.39

The material parameters are assumed to be constant in each element for both models.

4.5 CONSTRUCTION SEQUENCES

The majority of the formulation work was spent in developing the sequential construction algorithms. Each of the construction stages to be simulated was carefully analyzed. Then the theoretical developments from Chapter III were modified and the model was formulated.

4.5.1 in situ

The initial stress state in a media is generally assumed to be known. Equations 3.2 and 3.3 provide the means to reproduce the in situ stress in the simulation model. The finite element program provides a means to calculate the vertical stress with no additional formulation effort. The

soil mass is assumed to behave as a linear elastic body and the forces are derived from the gravity loading of the body. The horizontal stresses are then set equal to the vertical stresses multiplied by the coefficient of lateral earth pressure at rest. Shear stresses are assumed to be zero for all cases. If the ground surface is sloping, appropriate shear stress should be included. For horizontal ground surfaces the formulation will provide good representation of the in situ stress if the coefficient of lateral earth pressure at rest is known.

4.5.2 dewatering

Dewatering is the next stage of sequential construction considered. In Chapter III the time dependent and coupled nature of the dewatering problem was discussed. In order to provide an economical formulation a very crude approximation of the dewatering process will be formulated. Both the coupling effects and the time effects are neglected.

The only effect of dewatering accounted for is the increase in the effective weight of the soil. This increase is accounted for by a body force within an element which has been dewatered. The body force is taken to be the unit weight of water. The equation below represents the method

of calculating the body force.

$$\{F\} = \int_{V'} \gamma_w [N]^T dV' \quad \text{Eq. 4.40}$$

Where

$\{F\}$ = nodal forces

γ_w = unit weight of water

$[N]$ = interpolation function matrix

V' = volume of dewatered element

Note that equation 4.40 applies only to elements which were submerged during the stage before and are now above the water table. No loads are generated by a decrease in pore water pressure alone. In Figure 5 only elements 1, 2 and 3 have body force loads due to dewatering. The remaining elements are affected indirectly by the loading from these three elements. The material parameters of dewatered elements may be changed also. While the formulation neglects many important features of dewatering, it does provide an approximate solution to the problem. For some problems dewatering may not be the critical step and therefore the proposed formulation can provide a reasonable answer at an economical cost.

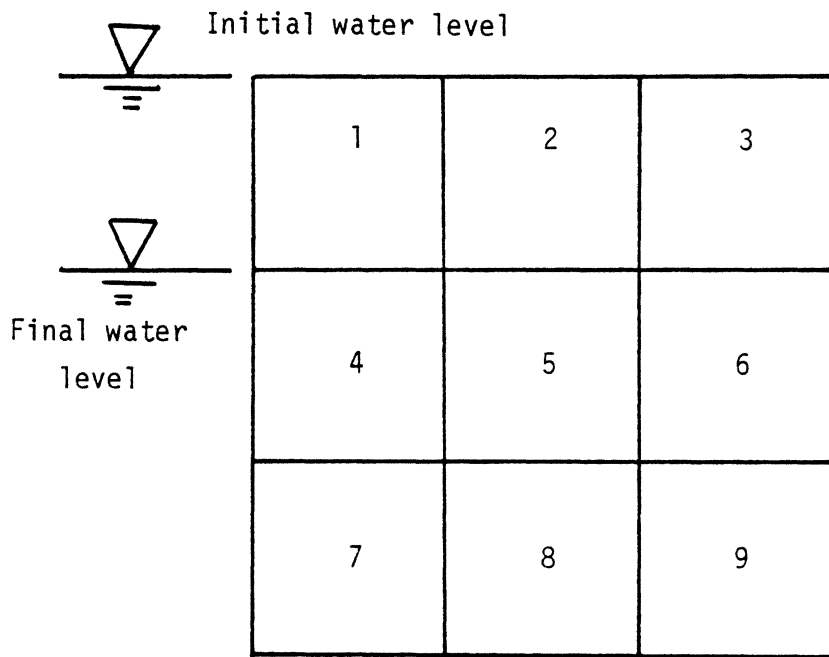


Figure 5: Example of Dewatering Mesh

4.5.3 excavation

The process of excavation requires careful formulation in order to obtain reasonable answers. The basic requirement of the problem is that the excavated surface be stress free. Also, due to the nonlinear material involved, the thickness of the layer removed at each step must be fairly small.

The quadratric element generally allows a more accurate fulfillment of the stress free boundary requirement as compared to lower crder elements. A quadratic element can have one boundary with zero stress while other boundaries have some finite stress. Linear elements have constant stresses throughout and therefore to obtain a stress free boundary the entire element must have a zero stress state. The basic algorithm for excavation is described below:

1. The initial stress state of the body is obtained.
2. The elements to be excavated are deleted from the system.
3. Iterations are performed until equilibrium of the remaining elements is obtained and a stress free boundary is approximently obtained.
4. Repeat steps 2-3 for each lift.

Two key features of the excavation routine are the fact that excavated elements are completely removed from the system and that the stress free surface is obtained by satisfying equilibrium. The equation used for calculating the nodal forces in an element due to the element's stress state is:

$$\{F\} = \int_v [B]^T \{\sigma\} dV \quad \text{Eq. 4.41}$$

Where

$\{F\}$ = nodal force vector

$[B]$ = displacement strain transformation matrix

$\{\sigma\}$ = vector of stresses

Summing all the forces calculated by equation 4.41 for each elements and adding to the applied forces leads to a global residual load vector. This load vector reflects the degree to which the element assemblage is not in equilibrium. Equation 4.41 provides the basis for the iterations to find the equilibrium and corresponding stress free surface of the body.

The use of an quadratic element and the consistent method for calculating the equilibrating load vector can be considered fairly new. Some of the merits of these features have been discussed by Clough and Manna (10).

4.5.4 deposition or embankment

The formulation of simulating embankment construction will be considered now. Embankment construction is the opposite of excavation. Simulation of embankment construction is considerably easier than excavation. The simulation of embankment construction is performed as follows:

1. The initial stress state is obtained
2. A layer of the embankment is placed.
3. The resulting stresses and displacements are calculated assuming the newly placed material has little strength.
4. Iterations are performed (if necessary) to obtain equilibrium.
5. The displacements of the surface of the embankment are set to zero.

6. Steps 2-5 are repeated for each layer.

The governing equation used to calculate the loads is given below:

$$\{F\} = \int_V \gamma_s [N]^T dV \quad \text{Eq. 4.42}$$

Where

$\{F\}$ = nodal forces

γ = weight of soil in the lift element

$[N]$ = interpolation functions

V = volume of lift element

Equation 4.42 is valid only for newly placed lift elements. The remaining elements in the assemblage are loaded indirectly by the new lift. The displacements at the top of each new lift are set to zero to simulate the fact that embankments in the field are usually brought to the proper elevation before a new lift is added.

4.5.5 tie-backs

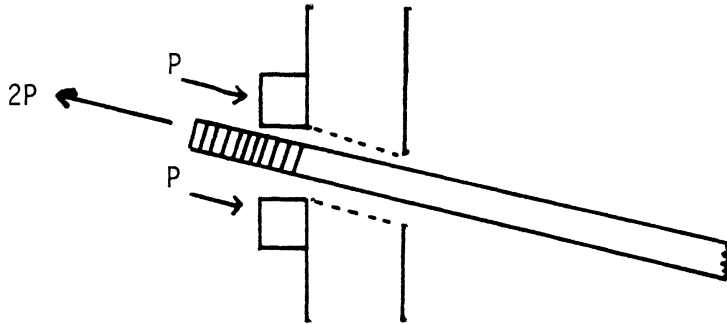
The major part of formulating tie-back simulation was done above when the bar elements were formulated. As stated in Chapter III, tie-back installation involves four steps. Boring the hole, placing the tie-back, grouting the tie-back and then tensioning the tie-back.

The boring of the hole will be neglected in this formulation due to the complex nature of the problem. The grouting process will be ignored for the same reason. The actual processes in tie-back installation as formulated are:

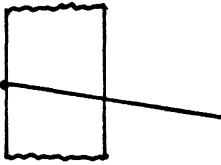
1. Apply a force along the direction of the tie-back equal and opposite to the tension force in the tie-back.
2. Solve for the new stresses and displacements.
3. Add the bar elements which make up the tie-back.
4. Set the bar element stresses to the initial tension of the tie-back.

The order of these steps seems odd but a glance at Figure 6 will illustrate the reason clearly. If the bar elements were added before the tensioning force was applied, they would tend to resist the tensioning force.

Physical Picture

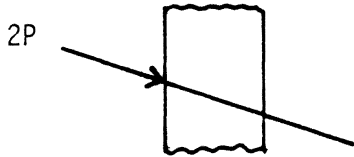
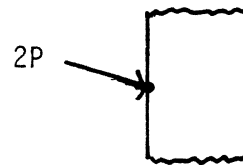


Wrong Sequence



Step 1

Correct Sequence



Step 2

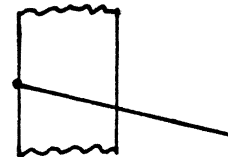


Figure 6: Tie-back Illustration

4.5.6 structural element placement

The placement of structural elements is the last construction phase considered. Structural element placement usually involves two steps. Removal of the geologic media where the structure is to be placed is first. Second is the placement of the structural element.

The present formulation does not account for the removal of the material where the structure is to be placed. What is formulated is to simply change the element constitutive law from one of soil material to that of structural material.

This simple formulation can be quite adequate for most problems. Consideration of the actual removal of soil is too expensive to be justified for most practical problems.

Chapter V

CODING

5.1 INTRODUCTION

Development of a code in order to model the process of sequential construction has been one of the major tasks in this thesis. The complex nature of the problem required a rather large program. Due to the size of the code, a large amount of time was needed to debug the program as subroutines were added.

5.2 PHILOSOPHY

Significant effort was expended to make the code both flexible and economical. At the same time, the input data was minimized and simplified. All of these factors are highly dependent on one another. Priority was given to making the input data as simple as possible.

Modeling sequential construction requires a great deal of input data just to describe the problem. By minimizing the data, the amount of user effort is decreased and correspondingly input errors are decreased. Although computational effort is increased, the program is more

economical due to the reduction in human labor. Flexibility of the code was considered to be the second most important factor. Because of new advances in the FEM, especially with regard to geomechanics, the ability of the code to be modified to include the new factors is important. Also the code's ability to be modified to model new construction sequences easily was considered important. At all stages of the coding, the program's computational efficiency was optimized within the limits of simple user input data and code flexibility.

The various features of the code are not new or original. However, the use of all of these features in a simulation program for sequential construction may be considered to be fairly unique. All of the features which will be discussed below, either contributes to the ease in data input, program flexibility or program efficiency.

5.3 FEATURES OF PROGRAM

Dynamic dimensioning of the arrays used in the code contributes to computer efficiency. By changing two lines in the code both small and large problems may be solved efficiently. An equation is provided to enable the user to set the array size. Arguments of the equation are the

number of nodal points, the number of elements and the maximum front width. The number of nodes and elements are self explanatory. The maximum front width quantity is related to the solution scheme used and will be discussed in detail below. By tailoring the array size to the problem the region requirements for a problem are minimized and therefore the cost of the computer run.

The computer code is quite modular in design and utilizes numerous subroutines. The use of a large number of subroutines reduces the amount of duplicate coding and allows for ease in adding or deleting various features of the code. For example, to obtain a highly efficient code for modeling excavation only, all that is required is to delete the subroutines dealing with other phases of construction. In the same manner, subroutines may be added to model the construction of reinforced earth retaining walls or frozen earth tunneling techniques (43,36,53).

The frontal solution technique developed by Irons (35) is used. Its use results in both increased efficiency (35,34) and a reduction in data preparation effort. The technique is based on Gaussian elimination which is optimized for use in conjunction with the FEM. Its unique feature is that

degrees of freedom are eliminated as soon as their corresponding stiffnesses are (fully) assembled. The result is reduced core storage requirements since the total global stiffness matrix is never present at one time. Other techniques such as the band-width method require that the total global stiffness matrix be assembled before the solution process begins. One result of the special solution process is that the nodal numbering has no effect on the time required for solution. Other solution techniques are directly dependent on nodal numbering for their solution efficiency. However, the frontal solution does require that elements be numbered in a special manner. The maximum front width is a measure of how well the elements have been numbered. By minimizing the maximum front width, optimum solution efficiency can be obtained. To calculate the front width the following algorithm may be used:

1. Loop through each element, (M) in numerical order.
2. For each element (M) find the number of nodes, (I) which are attached to both elements numbered lower than M and elements numbered higher than M.
3. Take IMAX to be the largest I found.

4. The maximum front width (MFRON) is then equal to IMAX plus the number of nodes in the element corresponding to IMAX, (NNE) all times the number of degrees of freedom, (DOF) in the problem.

The equation is as follows:

$$\text{MFRON} = (\text{IMAX} + \text{NNE}) \text{DOF} \quad \text{eq. 5.1}$$

Numbering the elements to obtain a minimum front width is much easier than numbering nodes in order to optimize other solution techniques. Another benefit is that the addition of elements to a mesh is merely a matter of renumbering the elements to retain optimum solution efficiency. Other techniques require renumbering the nodal points for retention of solution efficiency. Renumbering nodes also requires changing all of the element connectivity data.

A graphics subroutine which plots the input mesh is of great aid to the user. The routine is intended to provide an easy means of checking the input data relating to the nodal point data and element connectivity data. The routine plots the mesh and numbers both the nodes and the elements

on most standard plotters. Most errors in the nodal or element data may then be easily found by examining the plot of the mesh.

A data debugging code was also prepared in conjunction with the program. This code is a special version of the main code. Only the data for a problem is read in and then written out onto paper or at a terminal. No computations are done. The mesh plotting routine mentioned above is also utilized.

The use of a separate code which is much smaller than the main program allows the program to be run interactively at a computer terminal. Through the use of the debugging code interactively, error free input data may be prepared quite rapidly and economically.

5.4 CODING DIFFICULTIES

Coding the formulation required the surmounting of a number of difficulties. While the formulation of the model was quite precise, the translation of the formulation into FORTRAN code was at times not. The nonlinear nature of the problem was the reason for most of the difficulties. The formulation presents a set of equations which are to be

coded. These equations usually cannot be solved exactly and obtaining the the answer involves solving the problem several times. The number of solutions required for a problem depends on the degree of nonlinearity involved, the computer code and the accuracy desired. Another coding difficulty encountered was the handling of the changes in the domain for various stages of construction.

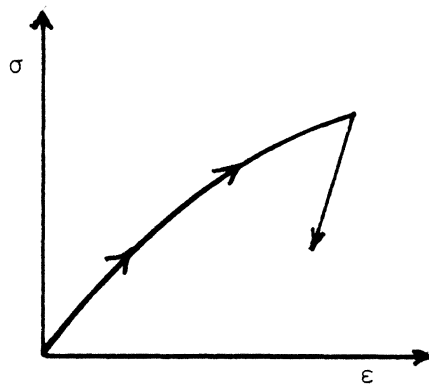
Nonlinear equations were solved by a combination of incremental and iterative approaches. Incremental solution techniques involve the application of the load in steps. A solution of each step is performed and the results are added to the previous results. This process is continued until the simulation is complete. The number of increments required depends upon the element mesh, the material behaviour and the degree of accuracy desired. Mesh dependency arises from construction steps involving excavation and embankments. The smallest load step possible for these cases depends on the size of the elements to be removed or added.

Iterations were coded to allow improvement of the agreement between the stress-strain state, the constitutive law and to obtain equilibrium. The Newton-Raphson technique

was used to handle the iterations. This method involves recalculating and resolving all the FEM equations for each iteration.

Incremental solutions are generally quite stable. However, a large number of increments are often needed in order to provide an accurate solution. The use of several iterations for each step allows the use of larger increments. This combination is usually the most economical although finding the proper combination of increments and iterations is difficult. In using the iterative approach, care must be taken for some loading paths. The iterations may actually diverge for some material models under certain conditions.

One aspect of material modeling which was particularly difficult to code was the unloading behavior of the soil elements. The problem arises from the relatively stiff response of soil as it is unloaded compared to the response as it is loaded. This feature is illustrated in figure 7. The figure shows representative stress-strain curves for unloading. Both the actual soil response and the response as predicted by various models are shown. If large increments are used the computations may be in great error.



Actual Soil Response

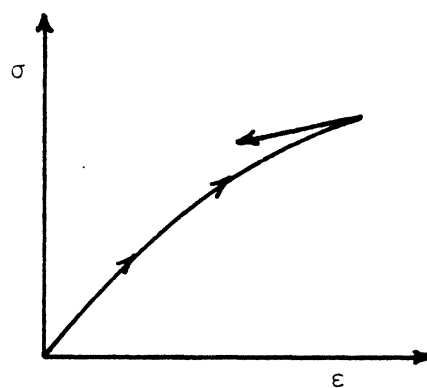
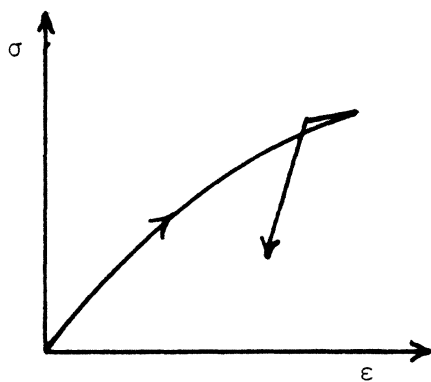
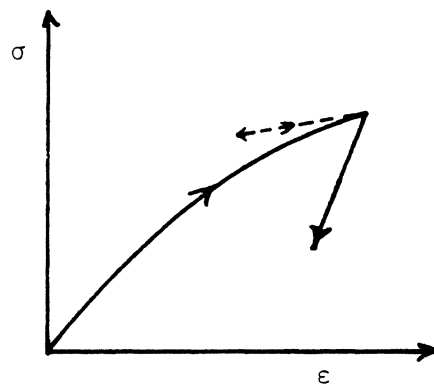
Response as Normally
Coded for Large
IncrementsResponse for Small
IncrementsResponse by Special
Modification

Figure 7: Unloading Stress-Strain Response

Small increments give better agreement between the model and actual responses. The cost of using small increments can be prohibitive. Therefore the method coded was the following:

1. Find the solution for the first increment.
2. Check for any elements which have unloaded for the first time during this increment.
3. Identify the newly unloaded elements.
4. Completely resolve for this increment using unloading moduli for the unloaded elements.

The effect of these steps is to find the elements which are going to unload and assign to them the proper material parameters.

Modification of the mesh at various stages in the simulation of sequential posed another coding challenge. The key to the solution of this problem was to read the entire mesh into storage initially. Then this mesh may be modified at each stage of construction to accurately portray the geometry.

Elements which are inactive do not enter into any of the calculations. This provides a more economical approach than

assigning a small stiffness value to reduce the deleted element's effect (9,40). By completely removing the element the set of equations becomes numerically more stable.

The coding was performed in such a manner that the nodes and elements to be deleted or added may be numbered in any order. The ability of random numbering makes it much simpler to prepare data and to make modifications in the data. Some computational efficiency was lost due to the need to check each element to see if it is active or not. The ability to have random numbering was considered to be more important than the small loss in efficiency.

The inactive elements are maintained in a numerical array. A subroutine is used to read the changes to the mesh and then to modify the array accordingly. A function subprogram is used to check for the existence of an element in the inactive array.

5.5 COMMENTS

Some aspects of coding the FORTRAN program SEQCON have been discussed. The resulting code stems from a great deal of trial and error work. The discussion above represents only a small, but important part of the knowledge gained from writing the program.

Chapter VI

VERIFICATION OF CODE

6.1 INTRODUCTION

A large number of problems were run utilizing the program SEQCON. The problems range from simple one element types to complicated sequential construction types. The purpose of all of these problems was to test and verify the capabilities of SEQCON. Three classes of problems were solved. First were the problems for which closed form solutions exist. Second were the problems with no solutions to compare them with. For these problems, only the trends were considered and the results were interpreted in a qualitative manner. The third group involved comparison with results from other numerical codes and field data. Discussion of the various problems is grouped by the complexity of the problem and the feature of the code it highlights.

6.2 GENERAL VERIFICATION

The first problem considered was a single element with a uniform loading. Figure 8 gives the geometry of the problem. This problem is basically one-dimensional and

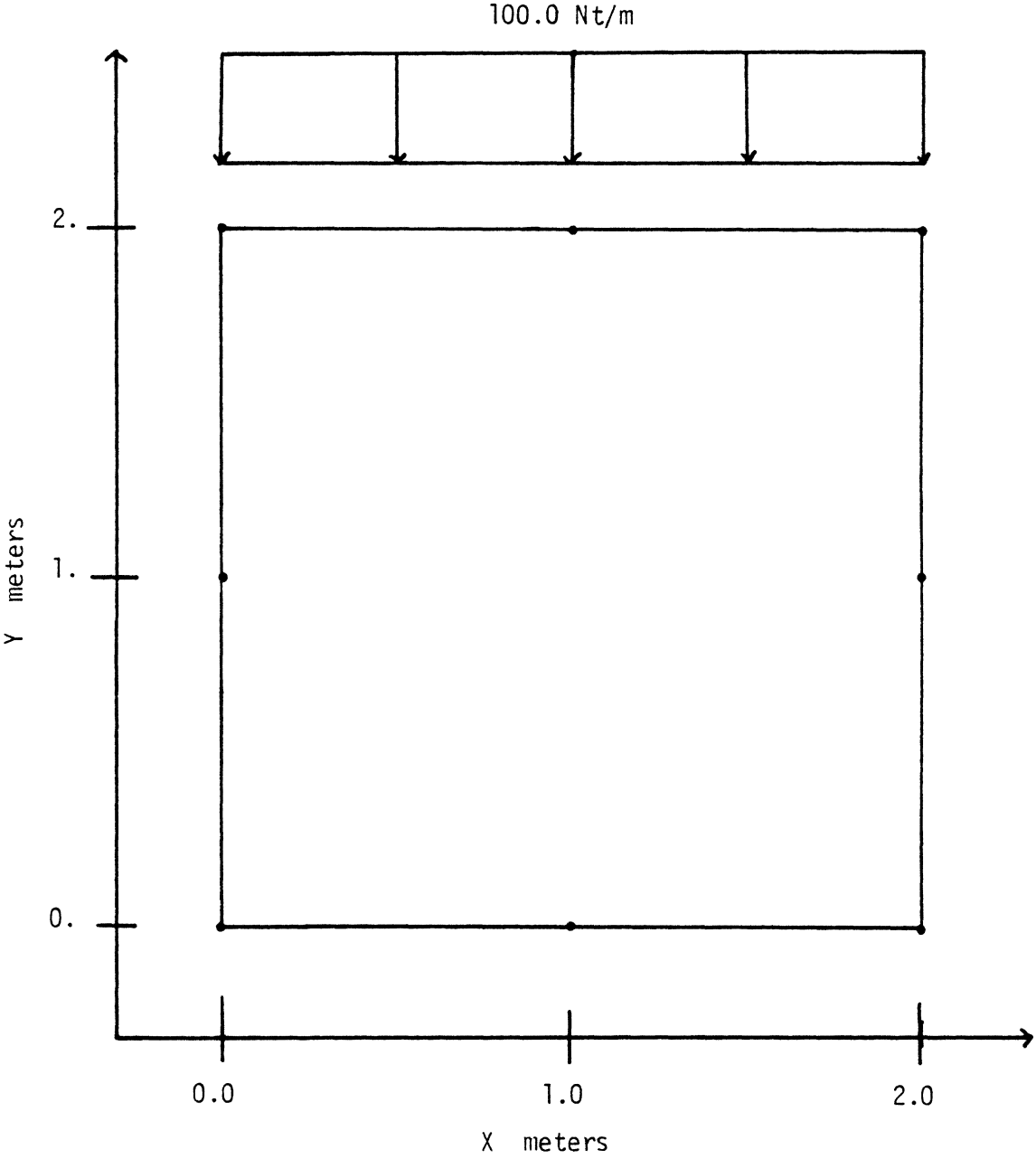


Figure 8: Single Test Element Mesh

provided the first verification of the basic code. Two runs of the problem were made using both a two-point and a three-point gaussian quadrature rule for integration.

The results are given in table 1 . The displacements compare well with the simple closed form solution for a one-dimensional body. It is interesting to note that the two-point integration gives more accurate results than three-point integration for this simple problem. Therefore, it appears that two-point integration should be used for regularly shaped elements under uniform loads.

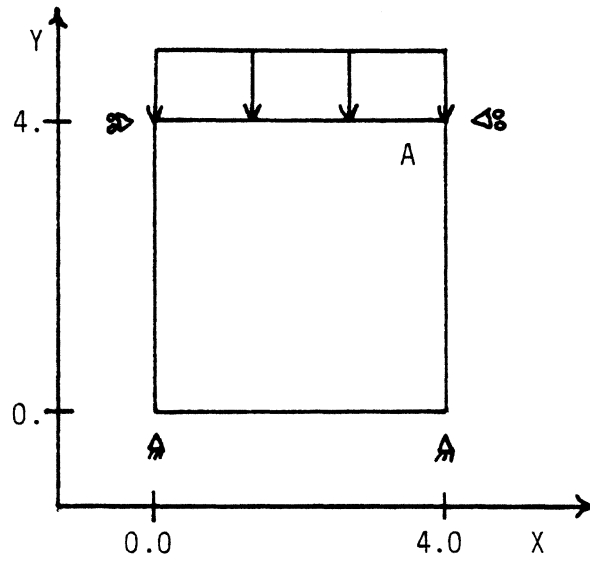
6.2.1 distorted element tests

The effect of element shape on the solution was explored next. Studies by Stricklin (54) and Taylor (55) indicate severe errors when distorted quadratic elements are utilized. The study presented here uses two problems to explore the effect of element shapes on the solution. The first problem considers a uniform load in a plane strain condition. The second problem uses the same mesh as the first but substitutes a point load for the uniform load. The geometry and loading of these two problems is shown in Figure 9 . Four different meshes were used to model both

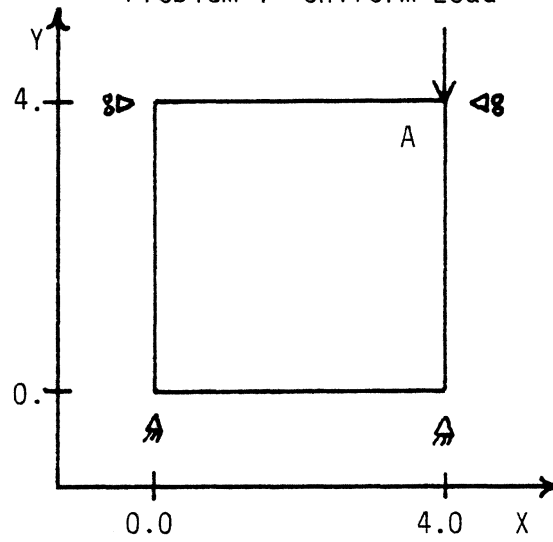
TABLE 1

Comparison of Two and Three Point Integration

solution type	stress in Y direction	displacement at Y = 2.0
closed form	100.0	-0.0002000
2 - point	100.0	-0.0001820
3 - point	98.5	-0.0001815



Problem 1 Uniform Load



Problem 2 Point Load

Figure 9: Distorted Element Geometry

problems. The mesh configurations are shown in figure 10 . The material was assumed to be linear elastic and the material parameters used were:

$$E = 3000000.0 \text{ Pa}$$

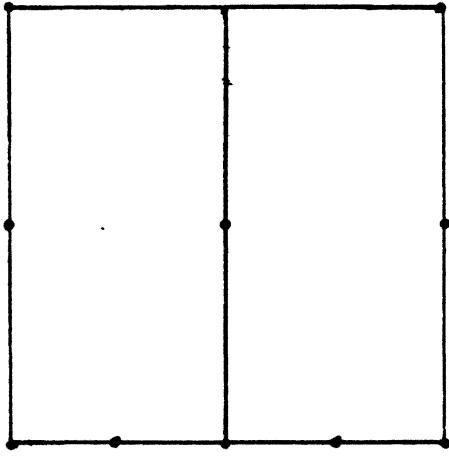
$$\nu = 0.30$$

Mesh I is assumed as the standard with which the other meshes are compared.

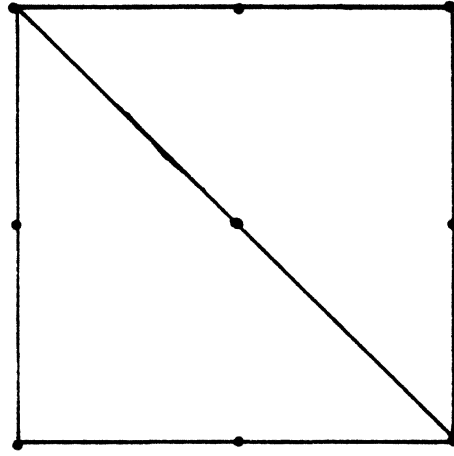
Table 2 compares displacements of one point for the various problems. These results indicate that for uniform stress states the shape of the element has almost no effect. Thus, it is possible to degenerate the quadrilateral into a triangle at locations of constant strain. The point load problems show large errors for distorted element meshes. It would appear that elements in areas of high stress gradients should be as rectangular as possible.

6.2.2 pure beam bending problem

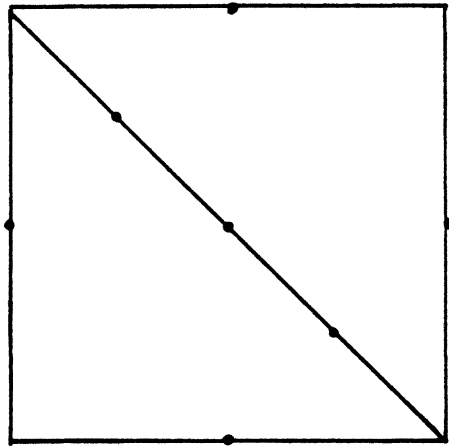
The problem of a beam in pure bending was modeled next. Plane stress conditions were assumed and the results are compared to those obtained by Desai and Abel (19 p.165) from



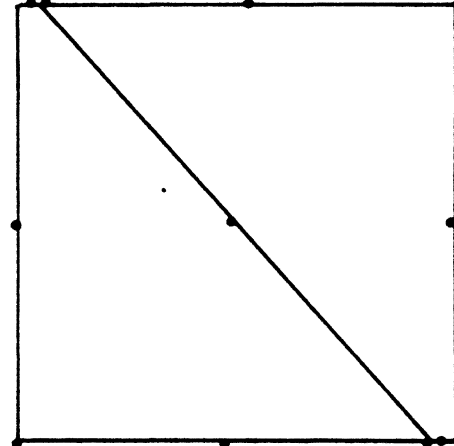
Mesh I



Mesh II



Mesh III



Mesh IV

Figure 10: Meshes for Distorted Element Tests

TABLE 2

Distorted Element Test Results

Mesh	Uniform Load Y Displacement at A m (X10 ⁻⁴)	Point Load Y Displacement at A m (X10 ⁻⁴)	% Error For Point Load
I	-9.90471	-9.99518	0.00
II	-9.90474	-7.05400	29.43
III	-9.90469	-7.64162	23.55
IV	-9.90474	-7.59990	23.96

a program utilizing four node quadrilateral composed of four constant strain triangles. Figure 11 illustrates the geometry and mesh for the problem. The following material parameters were used:

$$E = 30 \times 10^5 \text{ psi}$$

$$\nu = 0.30$$

$$\text{Thickness} = 1.0 \text{ inch}$$

The results are given in Table 3 Comparing the eight-node results to the four-node results demonstrates the greater efficiency of the higher order element. The SEQCON program yields results which are almost identical to the exact solution with a relatively coarse mesh. Additionally, this problem verifies the accuracy of the SEQCON program for linear elastic plane problems.

6.2.3 thick-cylinder problem

A check of the axisymmetric capability of the code was made by modeling a thick-walled cylinder. The cylinder is assumed to be of infinite length and the material properties are:

$$E = 1.0 \times 10^5 \text{ Pa}$$

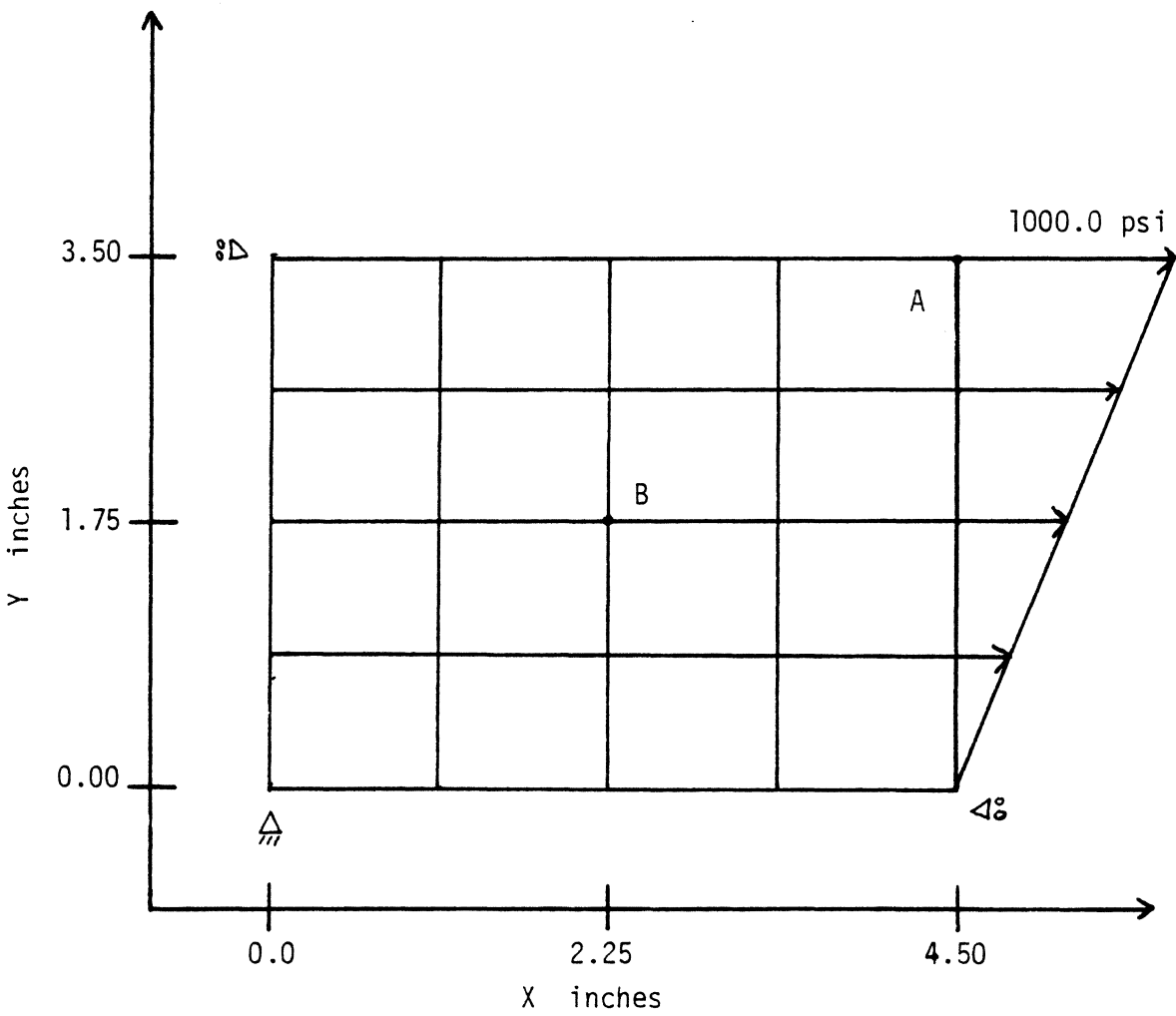


Figure 11: Pure Beam Bending Problem

TABLE 3

Results for Beam Bending Problem

Solution Type	Displacement in Inches ($\times 10^{-4}$)	
	Point A	
	X	Y
Exact	1.500000	-1.275000
Desai and Abel 25 Nodes 16 Elements	1.455171	-1.239908
Desai and Abel 81 Nodes 64 Elements	1.486224	-1.264569
SEQCON 65 Nodes 16 Elements	1.500100	-1.274930
Point B		
Exact	0.3750000	-0.3187500
Desai and Abel 25 nodes 16 elements	0.3679722	-0.3123025
Desai and Abel 81 nodes 64 elements	0.3732400	-0.3171139
SEQCON 65 nodes 16 elements	0.3750270	-0.3186380

$$\nu = 0.20$$

$$p = 1000.0 \text{ Pa}$$

A closed form solution from Popov (50, p. 418-419) is used for comparison.

$$\sigma_r = - \frac{pr_o^2}{r_o^2 - r_i^2} \left(1 - \frac{r_i^2}{r^2}\right) \quad \text{eq 6.1}$$

$$\sigma_t = - \frac{pr_o^2}{r_o^2 - r_i^2} \left(1 + \frac{r_i^2}{r^2}\right) \quad \text{eq 6.2}$$

$$u = \frac{1 - \nu}{E} \left[- \frac{pr_o^2 r}{r_o^2 - r_i^2} - \frac{pr_i^2 r_o^2}{r(r_o^2 - r_i^2)} \right] \quad \text{eq 6.3}$$

Where:

σ_r = Radial Stress

σ_t = Tangential Stress

p = External Pressure

r_i = Inner Radius

r_o = Outer Radius

r = Radius

u = Radial Displacement

The geometry, loading and mesh are illustrated in Figure 12 . Comparison of computed displacements and stresses with closed form solutions are given in Table 4 . The displacements of the inside wall of the cylinder are in error by 20 percent. The displacements of the outer wall of the cylinder are only in error by 4 percent. The computed and closed form stresses are in almost exact agreement. Considering the coarseness of the mesh the close agreement between the calculated and exact solutions indicate the validity of SEQCON for linear elastic axisymmetric problems.

6.2.4 hyperbolic test

The hyperbolic constitutive model behavior was investigated using a single plane strain element. A uniform surface load was applied. A confining stress of 20 pounds per square foot was used. The geometry of the problem is shown in Figure 13 . Material parameters used are given in Table 5 . These parameters represent a sandy soil with Poisson's ratio assumed constant. In addition to checking the hyperbolic model behavior, three different combinations of load increments and iterations were studied. First, nine load increments of ten psf each with no iterations was used (incremental method). Second, nine load increments of ten psf each with one iteration was used (mixed method). Last,

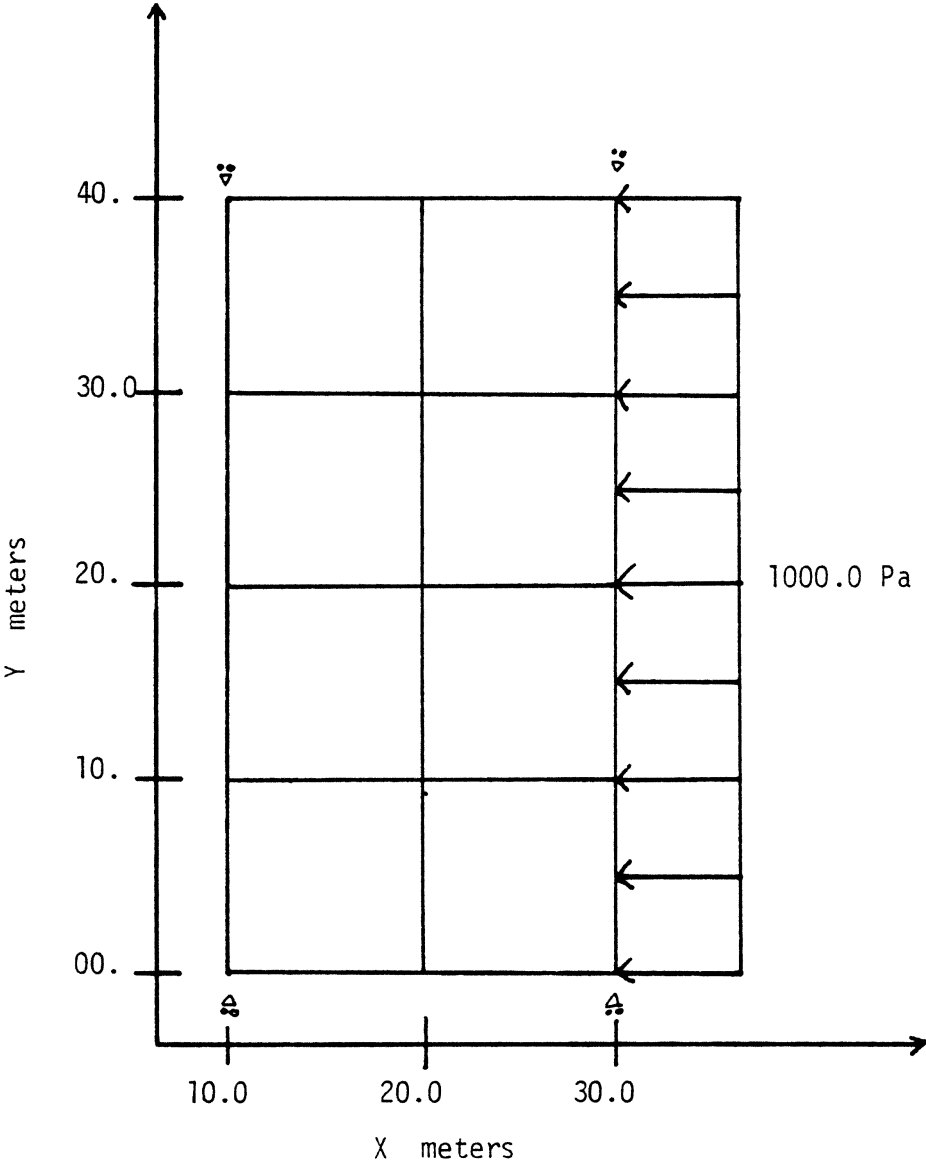


Figure 12: Axisymmetric Pressure Vessel

TABLE 4

Axisymmetric Problem Results

Solution Type	Tangential Stress Pa at r=12.11	Radial Stress Pa at r=27.89	Tangential Stress Pa at r=27.89
Computed	-1904.00	-980.80	-1269.00
Exact	-1892.12	-980.37	-1269.63
solution type	Radial Displacements m		
	at r=10.0	at r=30.0	
Computed	-0.216	-0.288	
Exact	-0.180	-0.300	

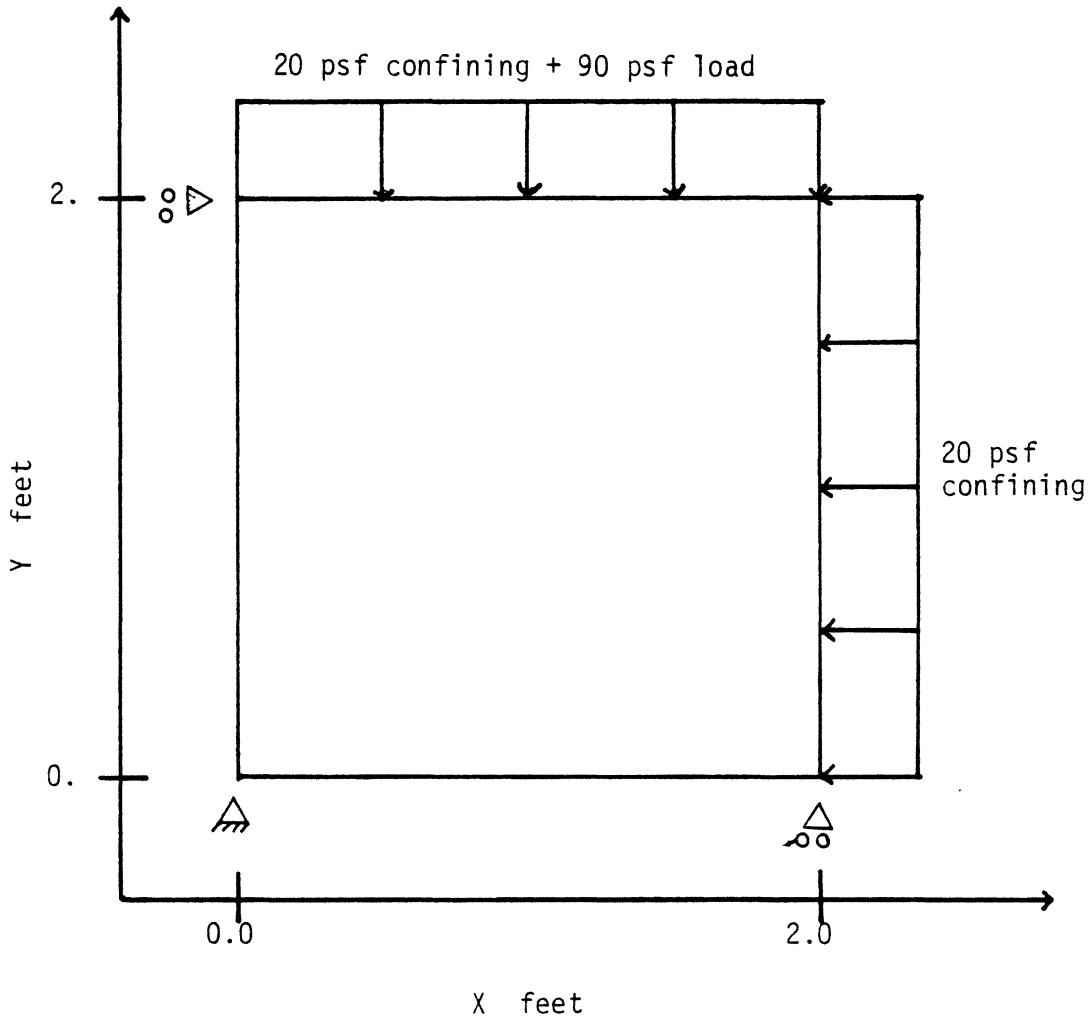


Figure 13: Hyperbolic Test Problem

TABLE 5

Material Parameters for Hyperbolic Test

$\nu = 0.30$	Failure Ratio	= 0.70
$\phi = 40.0$	Modulus exponent	= 0.50
$c = 0.0$	Modulus Factor	= 500.0

one load increment of 90 psf with nine iterations was used (iterative method). An exact solution was obtained using equation 4.11 . The results of these four solutions are shown in Figure 14 . From the graph it is seen that the element is loaded to failure. The solution utilizing one load increment and nine iterations provides the most accurate answer. It is also the lowest cost method. The incremental method gives the least accurate solution although it is fairly accurate for lower stresses. The mixed procedure provides a better solution than the incremental method alone especially as failure is approached. The iterative solution gave the best results for this particular problem. The results of this problem verify the hyperbolic coding and the solution techniques for nonlinear problems.

6.2.5 cap model test

A similar test problem was run for the cap type plasticity model. Here a single axisymmetric element is used. The geometry is given in Figure 15 . The problem is a one-dimensional type with the following material parameters:

$$E = 100 \text{ ksi}$$

$$C = 0.18$$

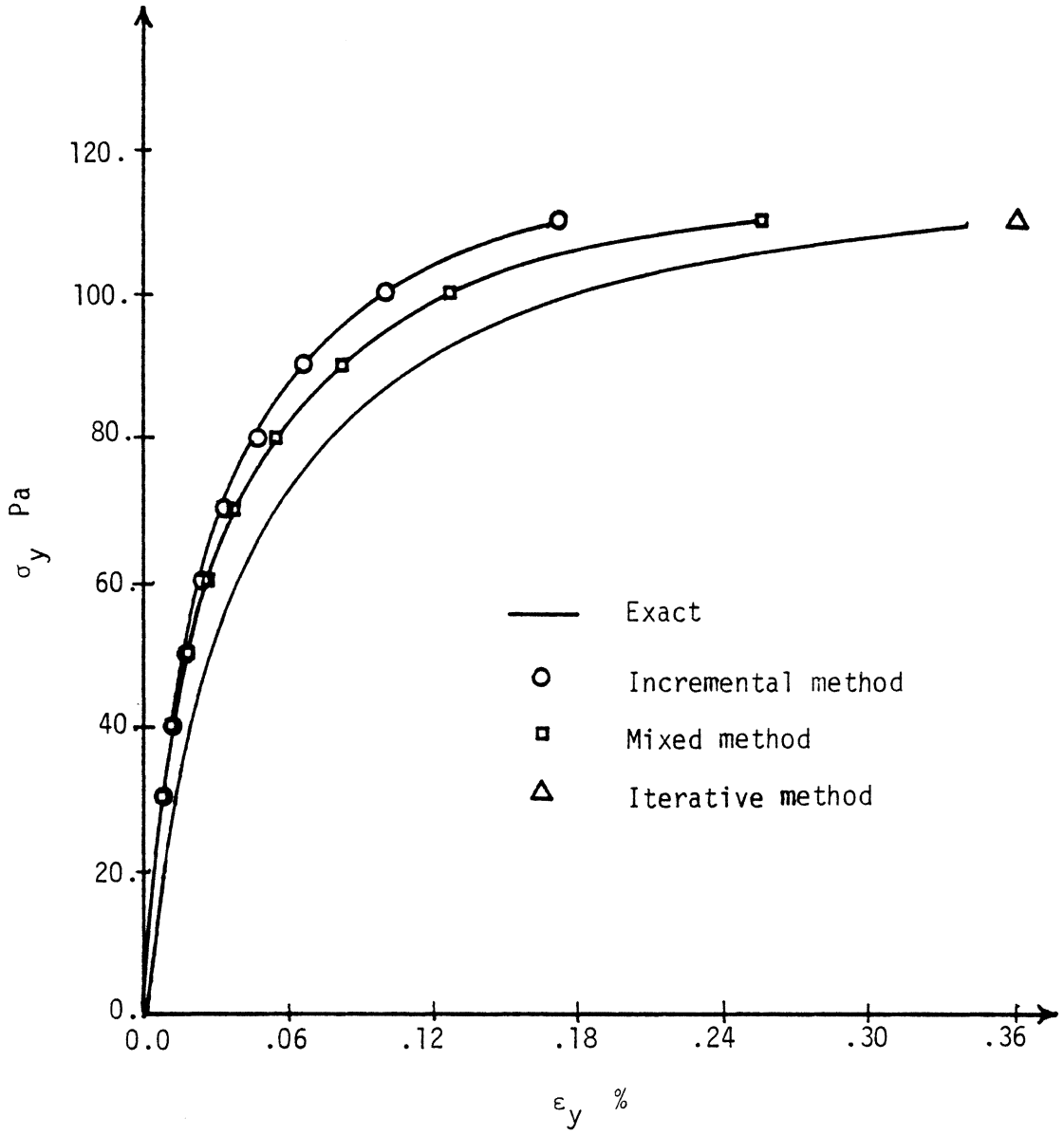


Figure 14: Hyperbolic Test Problem Results

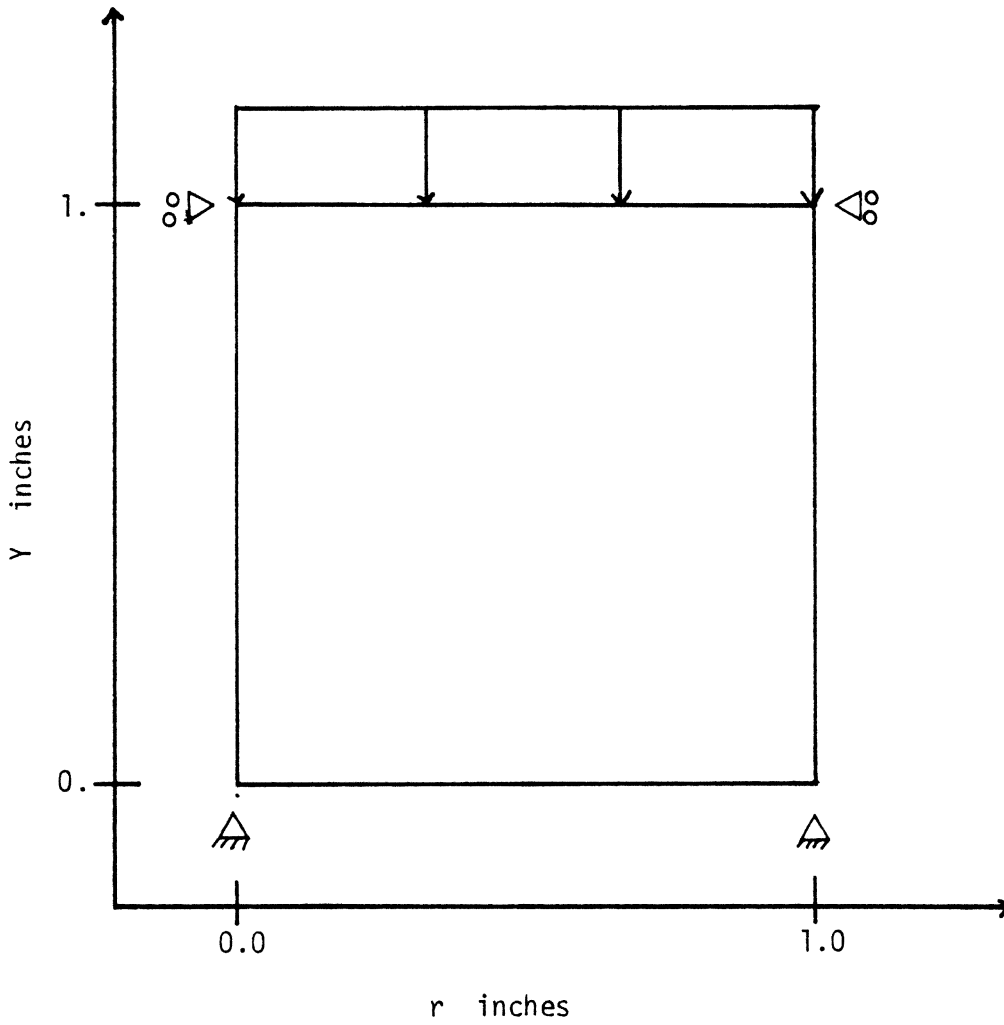


Figure 15: Cap Model Test Problem

$$\nu = 0.25$$

$$D = 0.67$$

$$A = 0.25$$

$$R = 2.5$$

$$B = 0.67$$

$$W = 0.066$$

Four load increments with six iterations per increment were used. The results are compared to those given by Sandler and Rubin (52) in Figure 16. The results were calculated by specifying the load or stress applied. This is in contrast to those given by Sandler and Rubin who specify the strain displacement and then calculate the stress. It is considerably more difficult to calculate strains if the stress is specified. However, for most geomechanics problems the loading is what is known not the displacements. The graph in Figure 16 shows that the calculated values from SEQCON are in good agreement with those of Sandler and Rubin.

6.2.6 bar element test

The bar element was checked through the use of the problem illustrated in Figure 17. The material parameter assumed are:

$$E = 30 \times 10^6 \text{ psi}$$

$$\text{Area} = 2.0 \text{ in}$$

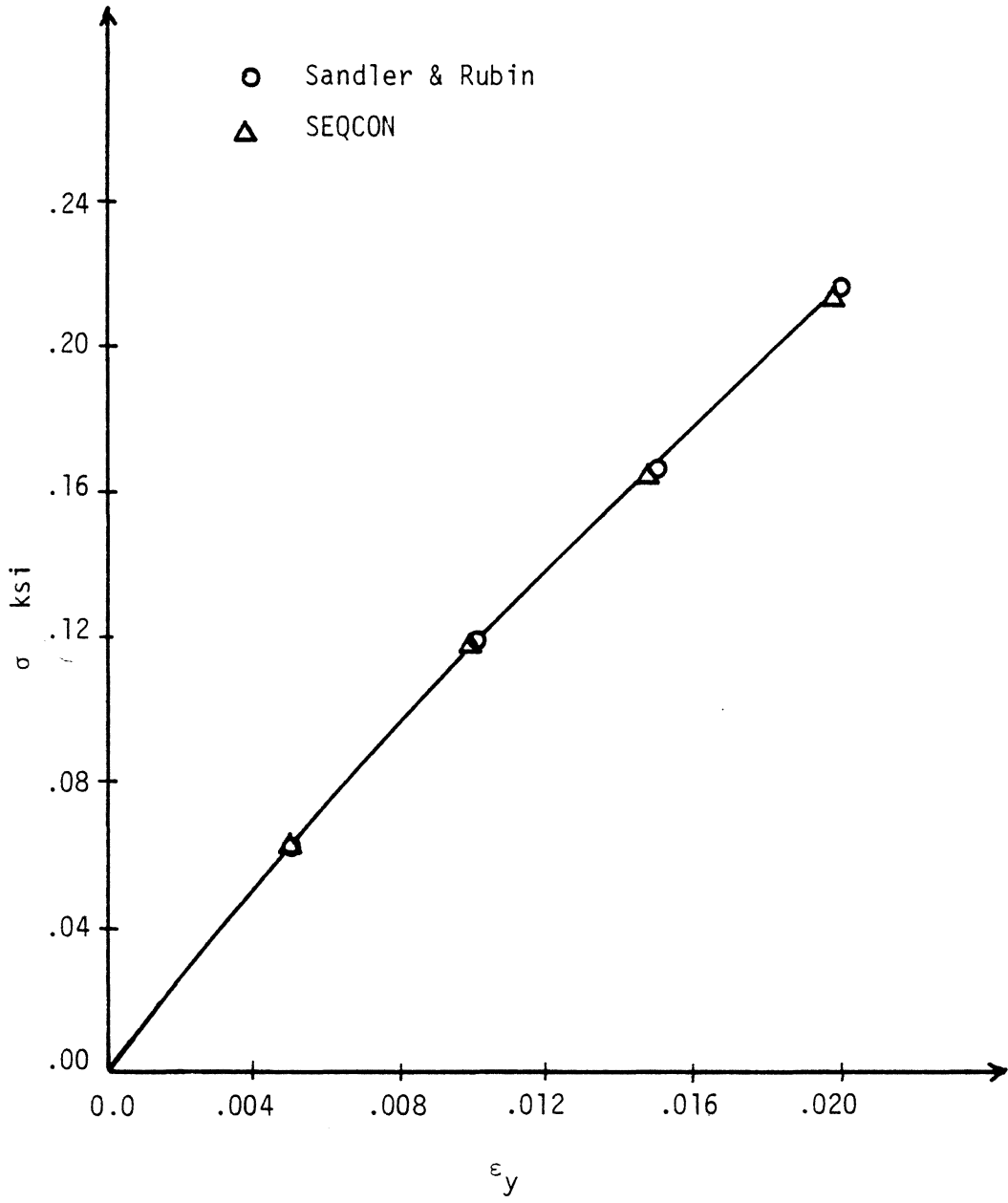


Figure 16: Cap Model Test Results

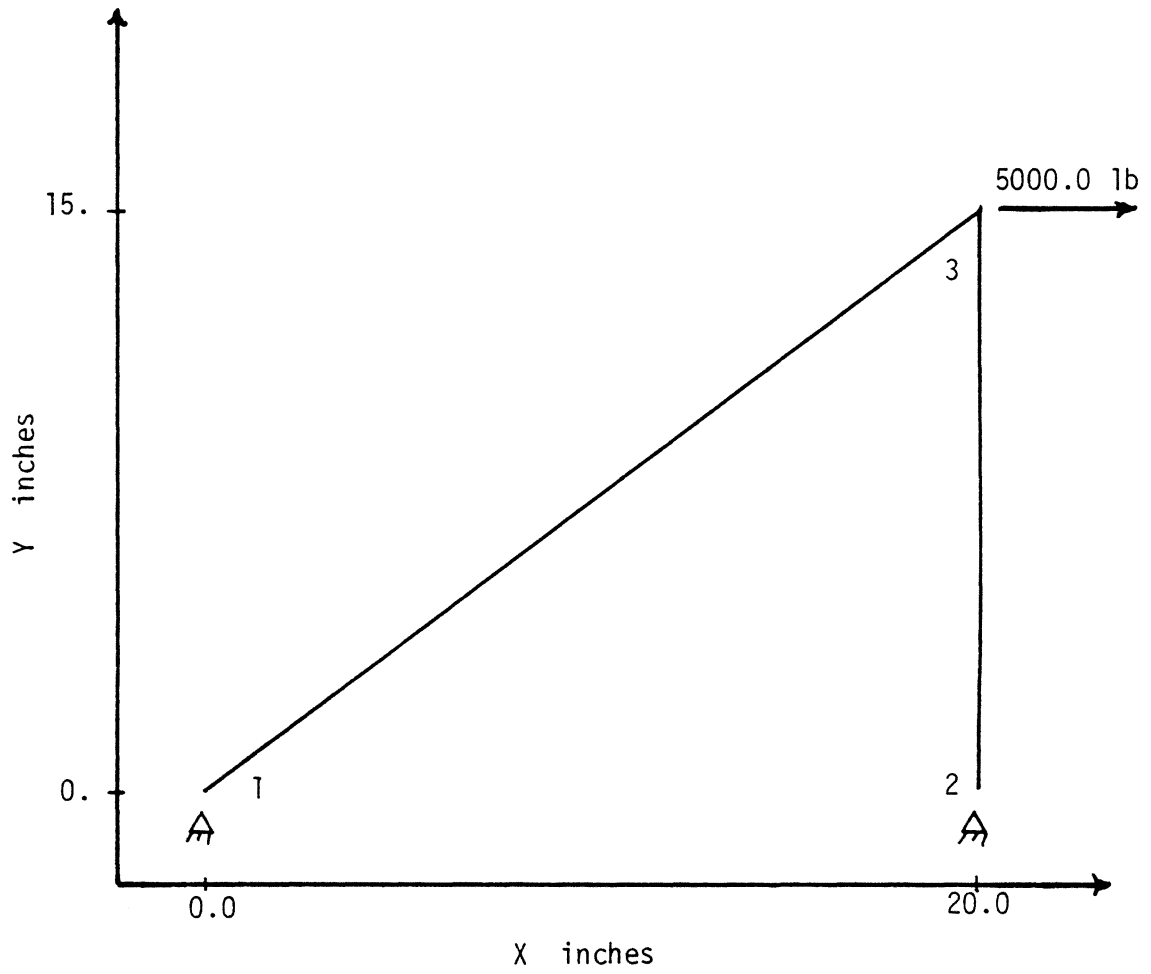


Figure 17: Bar Element Test Problem

A closed form solution was found using elementary mechanics and small displacement assumptions. As seen in Table 6, the calculated results are in exact agreement with the closed form solution.

6.2.7 interface element test

The next problem considered was a simple test of the interface element. The problem consists of a single interface element in pure shear. The geometry of the problem is given in Figure 18. The interface was considered to be linear elastic and the material parameters are as follows:

Normal Stiffness = 1000.0 Pa

Shear Stiffness = 10000.0 Pa

The computed horizontal displacement of 0.02 meters at point A is exactly the answer expected. The shear stress of 200.0 Pa is also exact. Thus for this simple problem the interface element appears to be correct. The next problem investigates some of the interface element's properties more closely.

TABLE 6

One-Dimensional Test Results

Solution	Stress psi		Displacement At Node 3 in ($\times 10^{-3}$)	
	Bar 1	Bar 2	X	Y
SEQCON	-3125.00	1875.00	3.95833	-9.37500
Exact	-3125.00	1875.00	3.95833	-9.37500

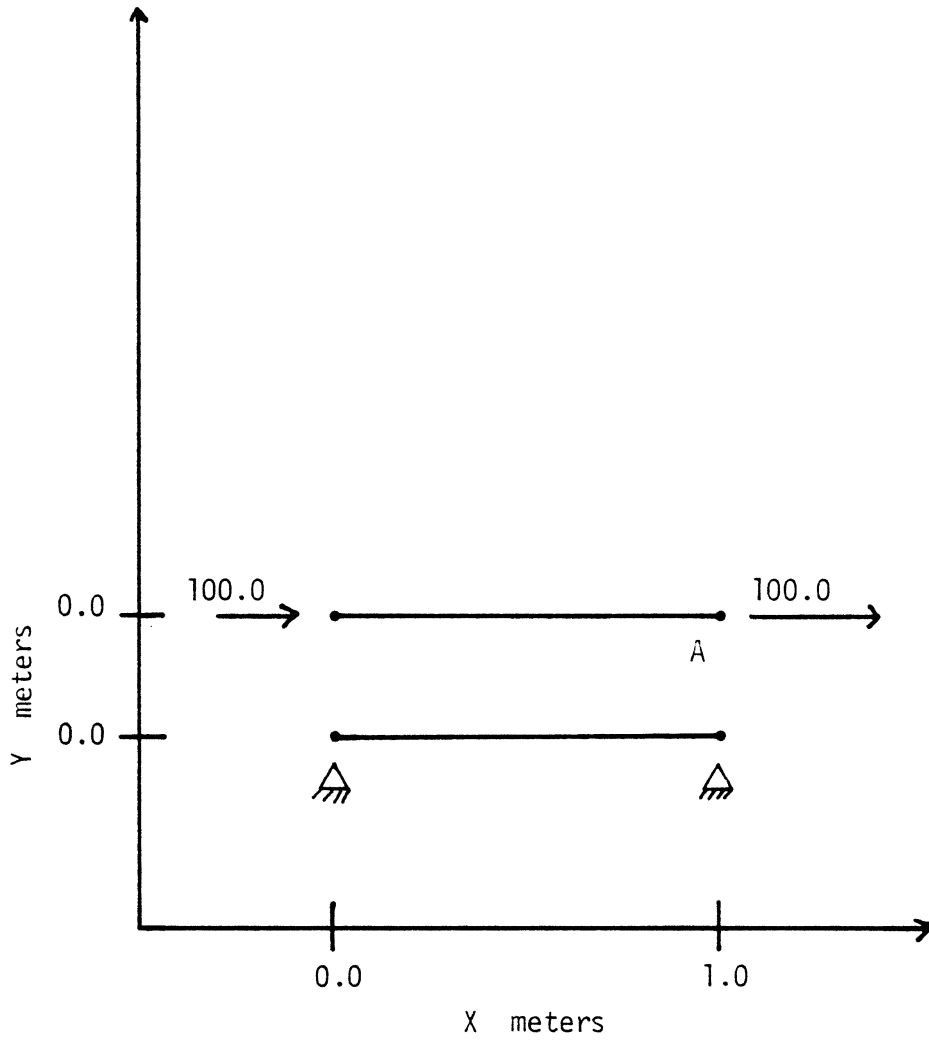


Figure 18: Interface Element Test Problem

6.2.8 soil-interface study

The following problem was devised to investigate the influence of interface elements on surrounding plane elements. Two interface elements are placed between two plane strain elements. The geometry is given in Figure 19 . Five problems utilizing different combinations of linear elastic interface material parameters were considered. The solid element material parameters are as follows:

$$E = 3.0 \times 10^6 \text{ Pa}$$

$$\nu = 0.30$$

The interface properties for the various cases is given in Table 7 . The results shown in Figure 8 are compared with the same problem with no interface elements as a control. The first three problems indicate that the results are independent of the value of the shear stiffness. This is what is expected due to the geometry and loading imposed. Problems IV and V indicate the importance of using a relatively high value for the normal stiffness. If the normal stiffness is too small, as in problem IV, the assemblage becomes too soft. The computed displacements are larger than the control solution and the calculated stresses are smaller than the control values. The higher normal

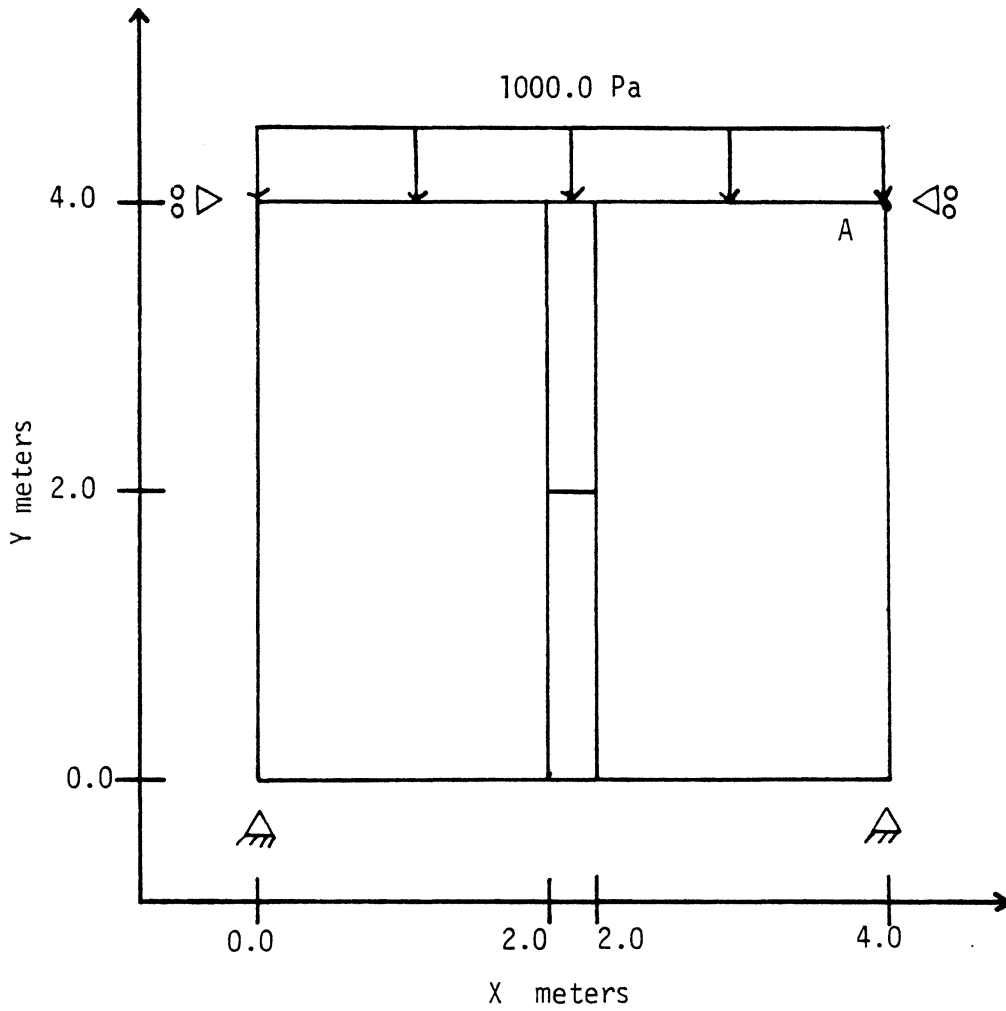


Figure 19: Mesh for Soil Interface Test

TABLE 7

Interface Parameters for Soil-Interface Test

Problem	Normal Stiffness Pa ($\times 10^6$)	Shear Stiffness Pa ($\times 10^6$)
I	3.0	1.15385
II	3.0	0.384615
III	1.0	3.46154
IV	1.0	1.15385
V	9.0	1.15385

TABLE 8

Results of Soil-Interface Test

Problem	Stress in X Direction Pa	Displacement in Y Direction at A m ($\times 10^{-3}$)
I	321.2	-1.068
II	321.2	-1.068
III	321.2	-1.068
IV	237.7	-1.131
V	382.4	-1.024
Control	428.6	-0.9905

stiffness in problem alleviates this difficulty to a large degree. This indicates that caution should be taken when using the interface element contained in SEQCCN. Choosing a relatively high value for the normal stiffness is in general a must for soil-structure interaction.

6.3 CONSTRUCTION SEQUENCES VERIFICATION

Initial verification and debugging of the construction sequences was performed using a simple nine element mesh. The problems were considered to be plane strain with linear elastic material properties. The problems considered were of a one-dimensional nature and the geometry and mesh are shown in Figure 20 . The material parameters are as follows:

$$E = 1.50 \times 10^{10} \text{ kg/m}^2$$

$$\nu = 0.3$$

$$\gamma_s = 2000.0 \text{ kg/m}^3$$

$$K_o = 0.50$$

$$\gamma_w = 1000.0 \text{ kg/m}^3$$

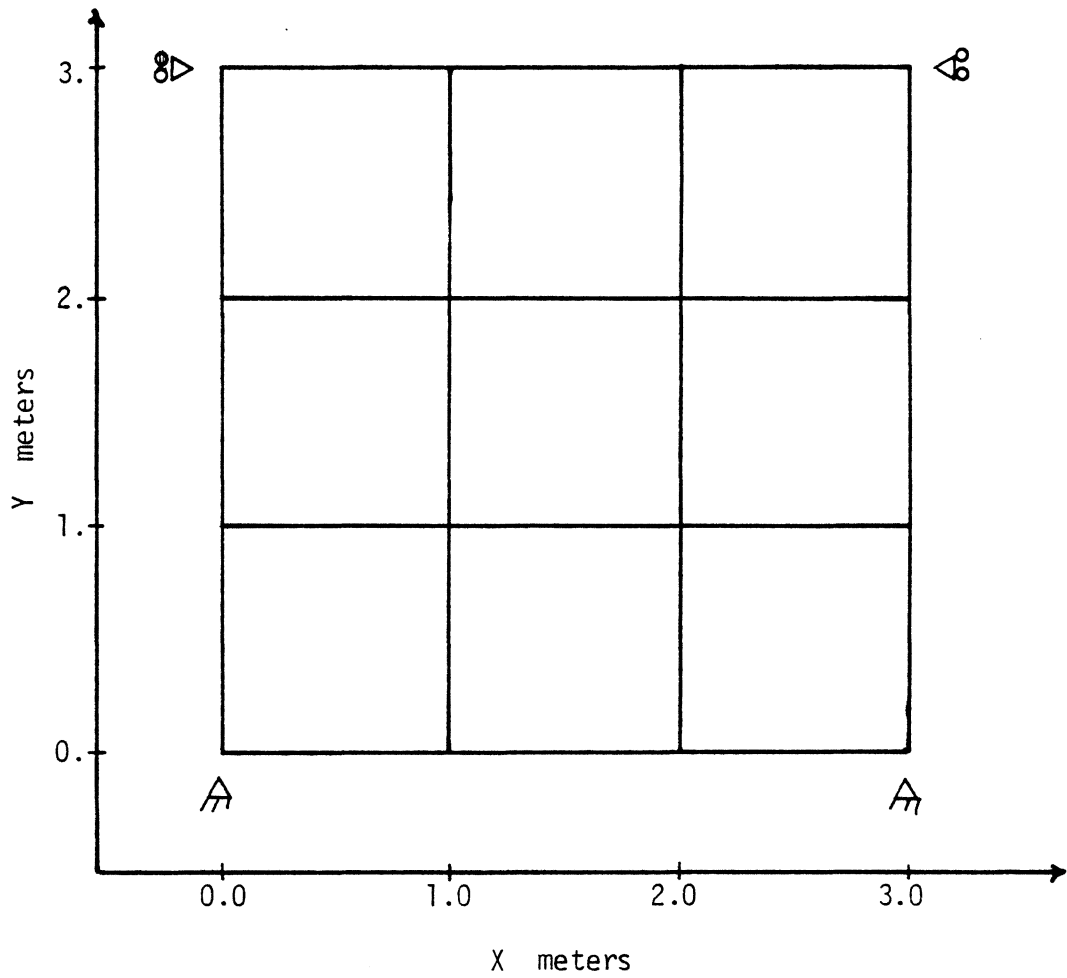


Figure 20: Ccnstruction Sequences Debugging Mesh

6.3.1 in situ

Initial stress calculations were the first construction step analyzed. Due to the homogeneity and one-dimensional nature of the problem equation 3.2 provides an exact solution. Figure 21 illustrates the correspondence between the exact solution and the computed results.

6.3.2 dewatering

A dewatering sequence was then analyzed. The geometry and mesh are identical to the above problem. The water table is initially at the ground surface. It is then lowered one meter and the stress and displacements are calculated. Figure 22 shows the correspondence between closed form solution and calculated results. Note that the closed form solution is based on the simple theory outlined in Chapter V for dewatering.

6.3.3 embankment

Embankment simulation was tested next. The mesh used in the two problems above was utilized by initially deleting the top three elements and then adding them back as an embankment lift. Material parameters are as above. The

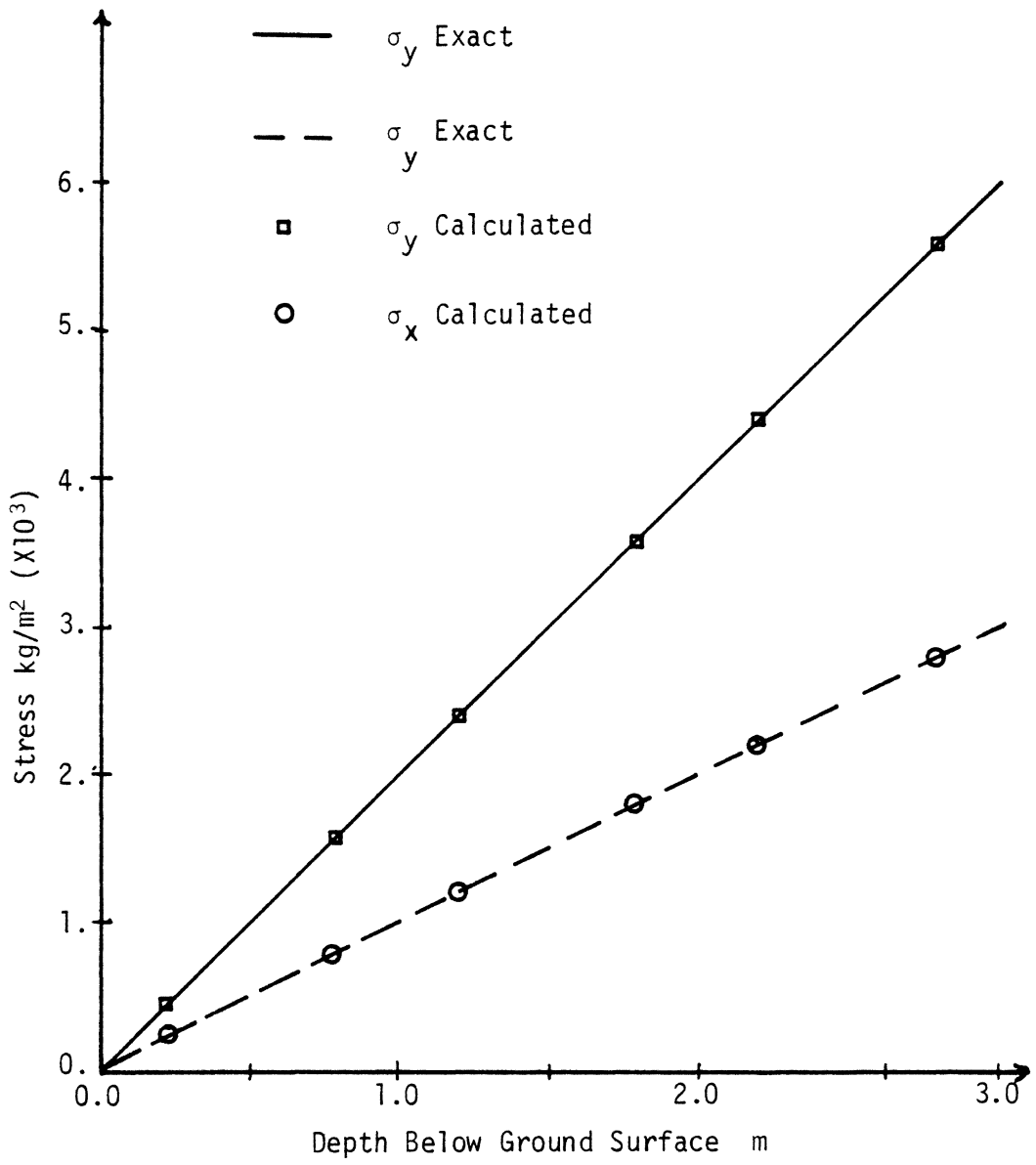


Figure 21: One-Dimensional Initial Stress Results

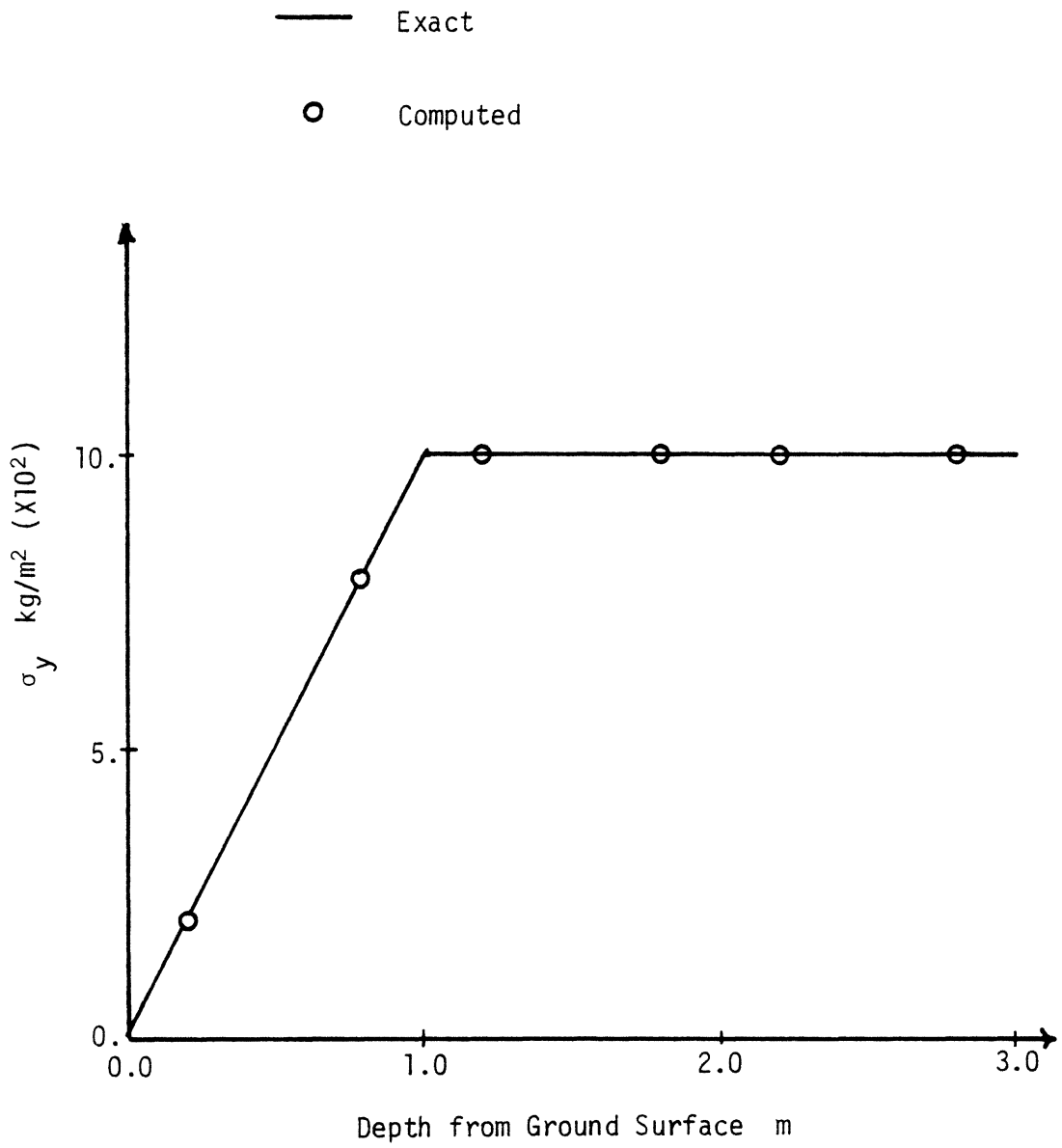


Figure 22: One-Dimensional Dewatering Results

computed results compare well with the closed form solution. In fact, the results are identical to those shown in Figure 21. This is the expected result due to the geometry and material properties assumed for this problem.

6.3.4 excavation

The last basic construction sequence verified with the simple mesh shown in Figure 20 is excavation. The top three elements in the mesh are removed as an excavation step. The results are shown in Figure 23. The stresses agree as well for the excavation sequence as for the other sequences.

The four simple problems above verify the validity of the basic construction sequences modeling routines. The following problems will examine more complex problems.

6.4 TIE-BACK WALL EXAMPLE

A more complex problem which modeled an excavation supported by a retaining wall will now be shown. The geometry of the problem is shown in Figure 24. Two analyses were made of this problem. The first analysis was made with out any tie-back support. The second analysis used a tie-back which ran from point A to point B. Point B

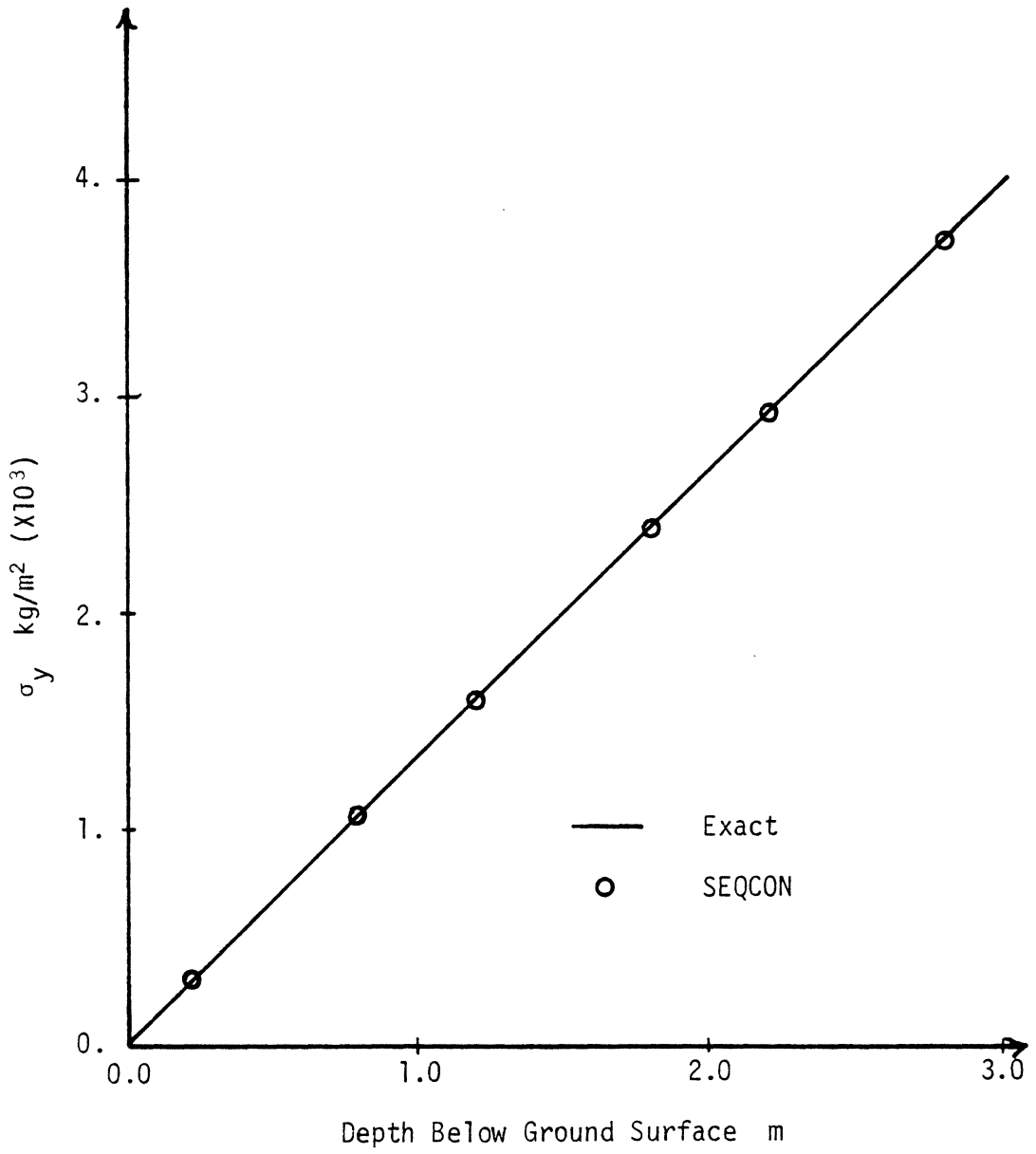


Figure 23: One-Dimensional Excavation Results

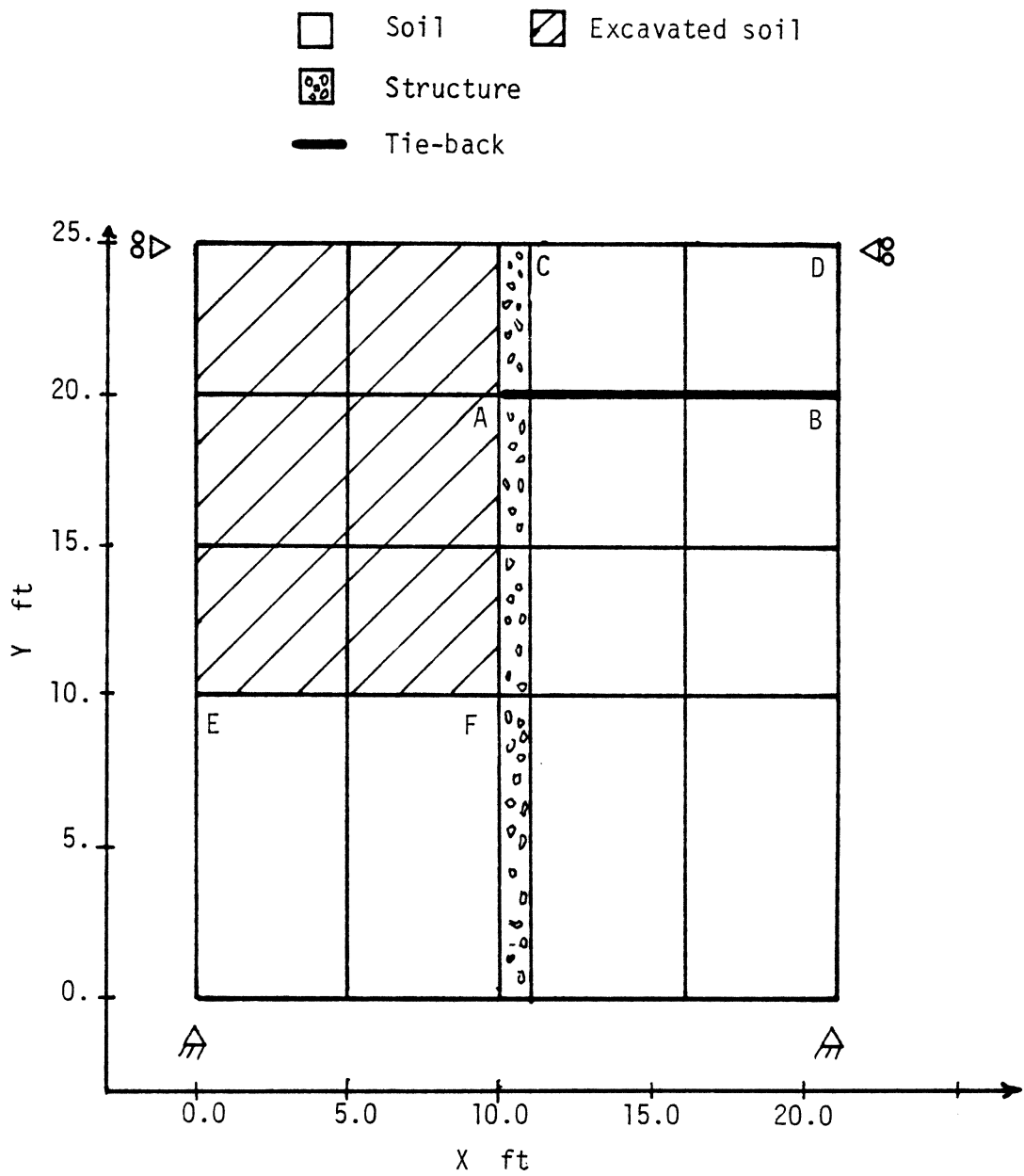


Figure 24: Simple Retaining Wall Problem

is assumed to be fixed in the X-direction. The tie-back was prestressed to 2000 pounds. Linear elasticity was assumed for each problem. The material parameters used for both analyses are given in Table 9. The excavation was carried out in three steps down to level EF. The tie-back was installed after the first excavation step.

Figure 25 compares the wall deflection of the analysis with and without the tie-back. The use of the tie-back actually pushed the wall into the soil mass. From this it can be ascertained that the initial tie-back tension was too great. The proper tie-back tension could be found through additional analyses using various values for the tension force. Figure 26 shows how settlements behind the retaining wall are reduced by the use of the tie-back. In this case the ground heaves due to the large initial tie-back loading. The absolute value of the ground surface movement has been reduced by approximately a factor of ten.

The results from this problem indicate the capability of SEQCON in simulating tie-backs. The next group of problems demonstrates the accuracy of the code in comparison with other numerical studies and with field data.

TABLE 9

Material Properties of Simple Retaining Wall

Parameter	Soil	Structure
E	20.0 X10 ⁵ psf	30.0 X10 ⁸ psf
v	0.45	0.30
γ	100.0 lb/ft ³	
K _o	0.50	
Tie-Back Properties		
E = 43.2 x 10 ⁸ psf		
Area = 0.025 ft ²		

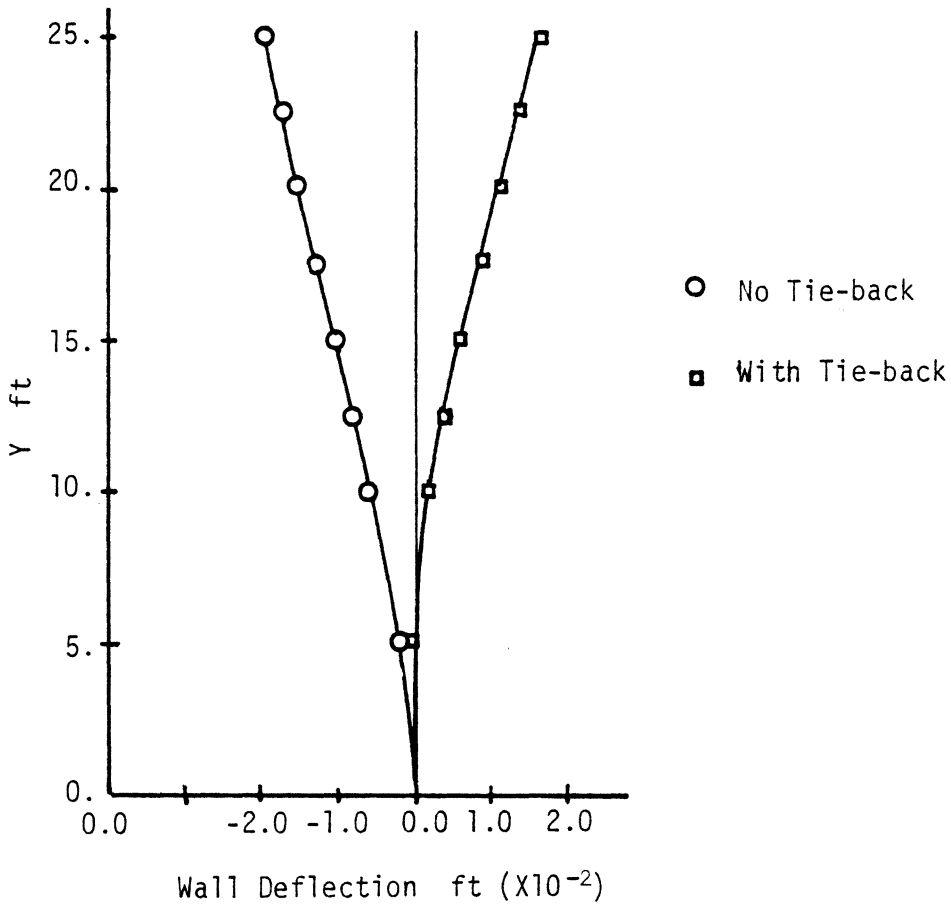
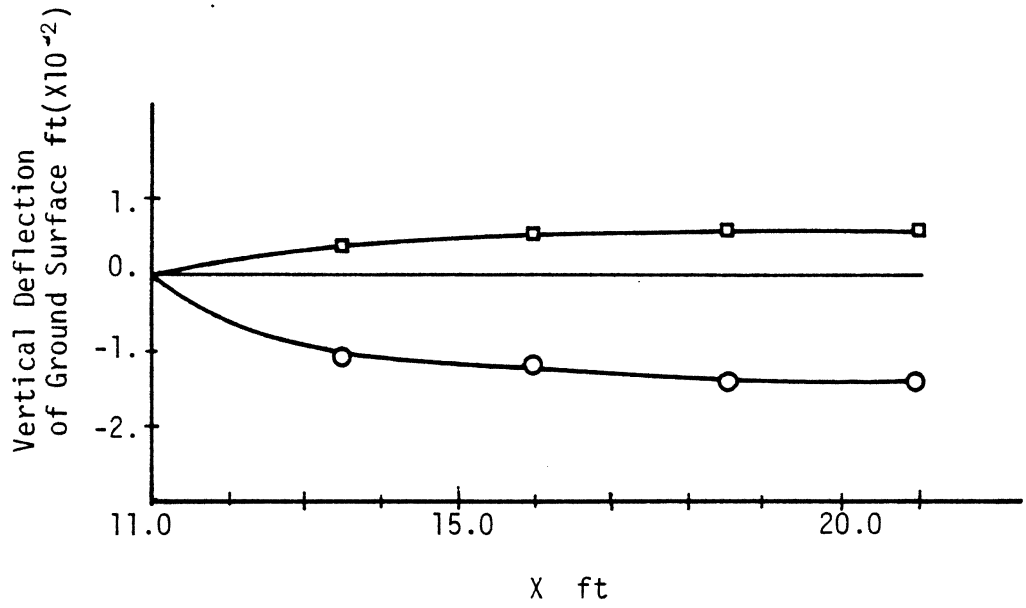


Figure 25: Wall Deflection of Simple Retaining Wall



○ without tie-back

□ with tie-back

Figure 26: Surface Settlement Behind Simple Retaining Wall

6.5 ADVANCED PROBLEMS

Three complex problems were solved to demonstrate the validity of SEQCON for more typical problems as encountered in the field. They are described in detail below.

6.5.1 footing problem

An infinite footing on a half space was the first practical problem considered. A mesh consisting of 21 elements and 84 nodes was used. The geometry of the problem is shown in Figure 27. The footing element was considered to be linear elastic and used the following parameters:

$$E = 4.0 \times 10^5 \text{ psi}$$

$$\nu = 0.30$$

The soil was modeled using the Drucker-Prager plasticity model. The material parameters are:

$$E = 4000.0 \text{ psi}$$

$$\nu = 0.35$$

$$\phi = 33.0$$

$$c = 0.35 \text{ psi}$$

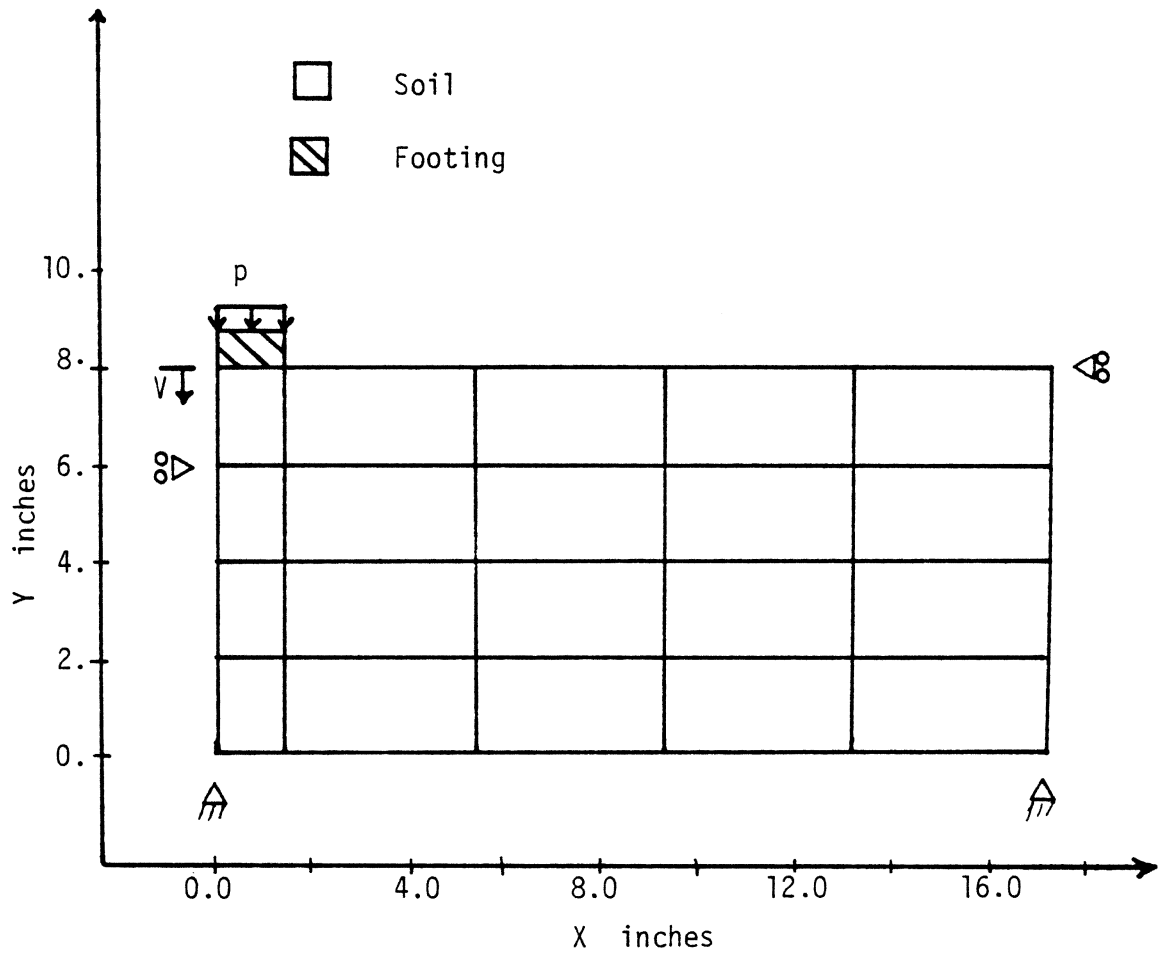


Figure 27: Footing Problem

The plane strain assumption is used to model the problem. The vertical displacement, V is compared with the experimental results given by Desai and Phan (22). A comparison of the results is shown in Figure 28. The computed results appear to compare poorly with the experimental data. Thus the Drucker-Prager model does not accurately represent the soil material. The reason is probably due to the model's inability to represent the volume change due to shear. The use of a cap type plasticity model would probably give better results.

6.5.2 dam with sequential embankment

An actual field problem analyzed was the construction of the Otter Brook Dam. An intensive analysis of the dam was made by Kulhawy, Duncan and Seed (42) and the problem data is adopted from their work. The dam itself was considered to be homogeneous and symmetric. Therefore only half of the domain was discretized. The dam was considered as a plane strain case. The geometry and mesh for the problem are shown in Figure 29. Table 10 gives the material properties used. The soil was assumed to follow the hyperbolic constitutive model. The mesh contained 42 elements and 153 nodes. Seven equal lifts were used with one iteration per lift.

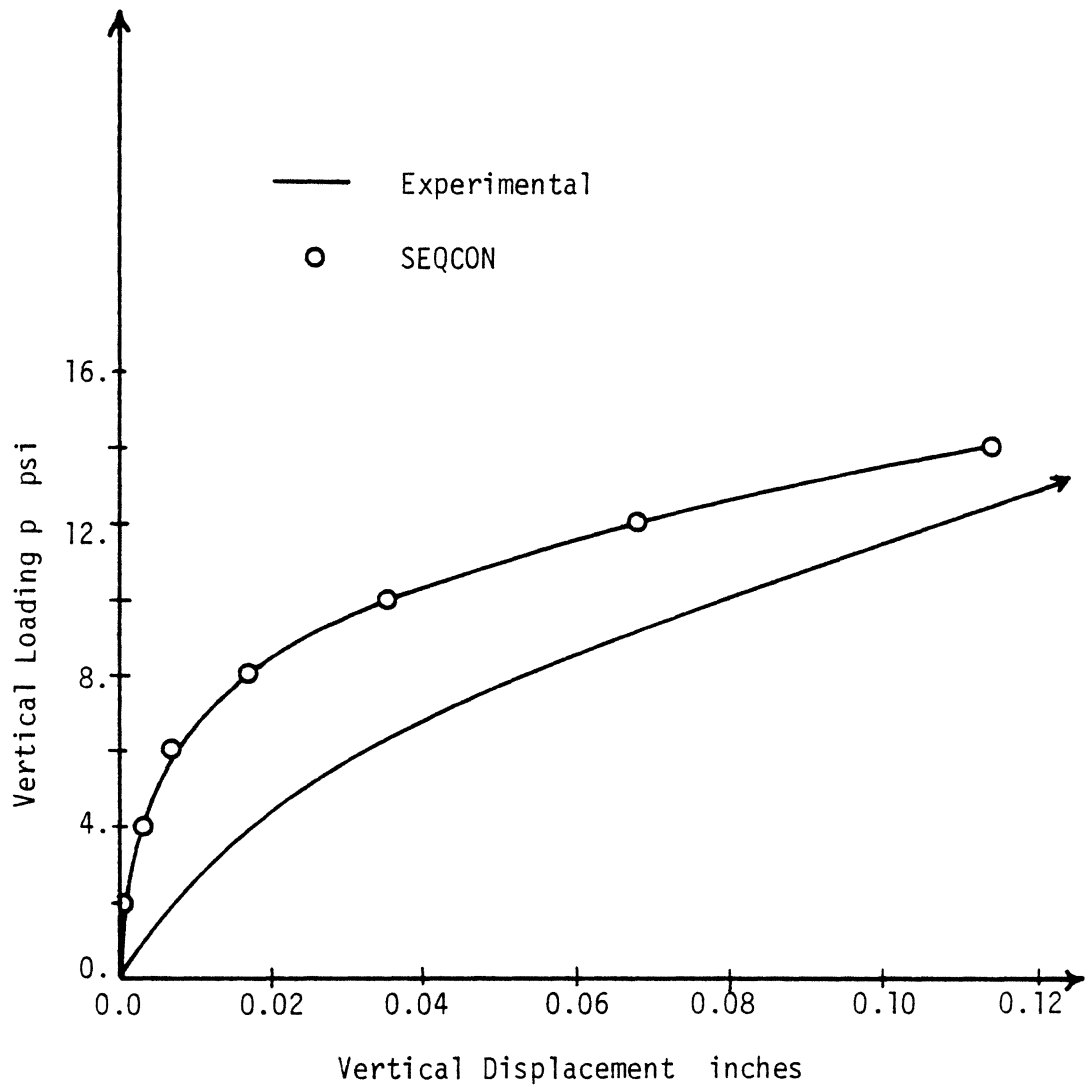


Figure 28: Load-Deflection Curve of Footing

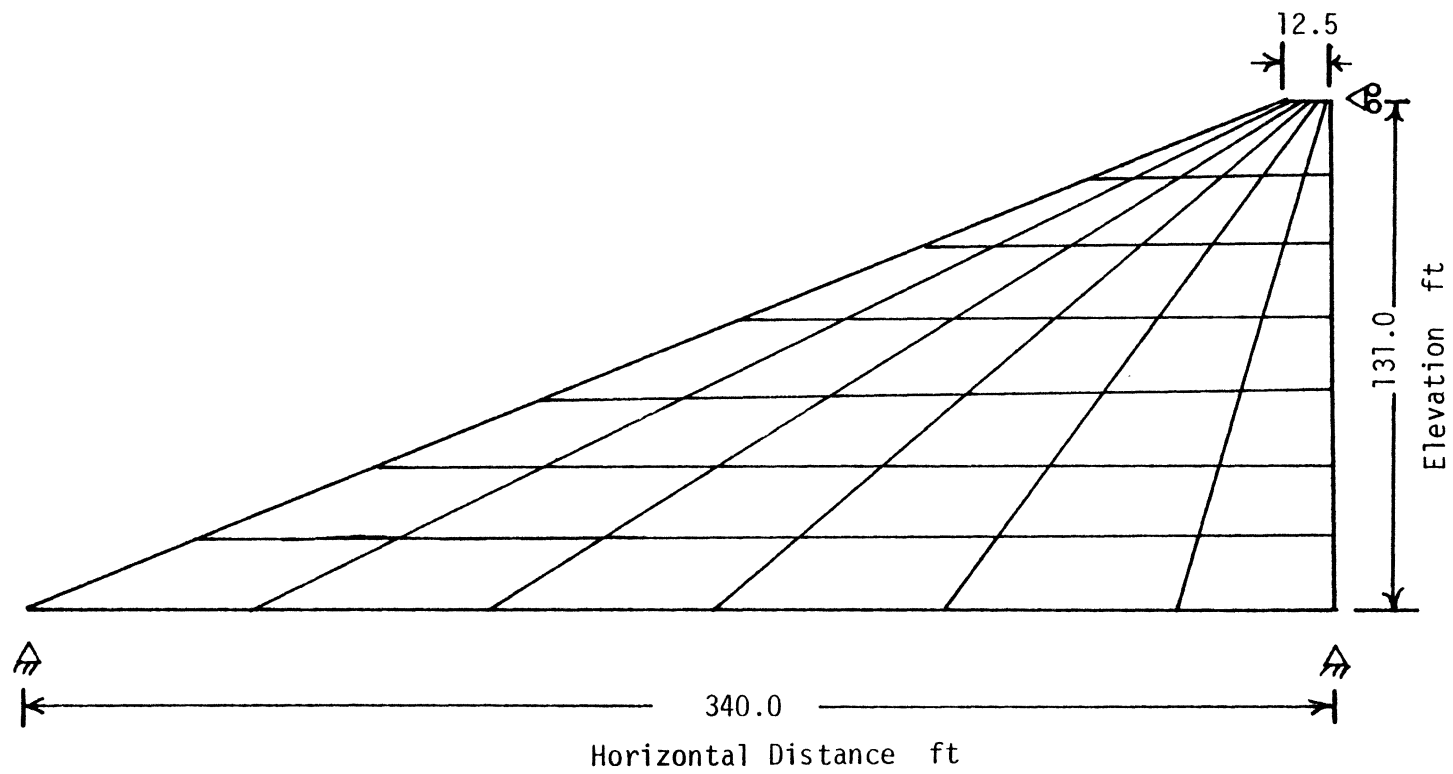


Figure 29: Geometry and Mesh for Otter Brook Dam

TABLE 10

Material Properties for Otter Brook Dam

Variable	Symbol	Value
Unit soil weight	γ_s	140.0 lb/ft ³
Cohesion	c	2160.0 lb/ft ²
Angle of internal friction	ϕ	14.0 degrees
Modulus factor	K	40.0
Failure ratio	R_f	0.68
Poisson's	G	0.43
Ratio	F	-0.05
Parameters	d	0.60

The computed results were compared with those found by Kulhawy, Duncan and Seed. The computed values obtained by SEQCON compared well with both Kulhawy, Duncan and Seed's results and with the field results. Figure 30 is representative of the accuracy of the calculated values. The figure plots the horizontal displacements of the upstream face of the dam. The good comparison of the displacements here indicates the overall accuracy of the computer model for this problem. This analysis illustrates the practical use of SEQCON for design and analysis of embankments.

6.5.3 retaining wall

A problem dealing with the passive resistance of soil to a retaining wall was the last problem analyzed. This problem is also analyzed by Matsuzaki (46). The problem consists of an infinitely long retaining wall. The wall is 3.05 meters high and the soil behind the wall extends for 10.7 meters. The soil is a medium-dense sand and the following hyperbolic material properties are used.

$$E = 48 \text{ mPa}$$

$$\gamma_s = 17.5 \text{ kNt/m}^3$$

$$\phi = 35.0 \text{ degrees}$$

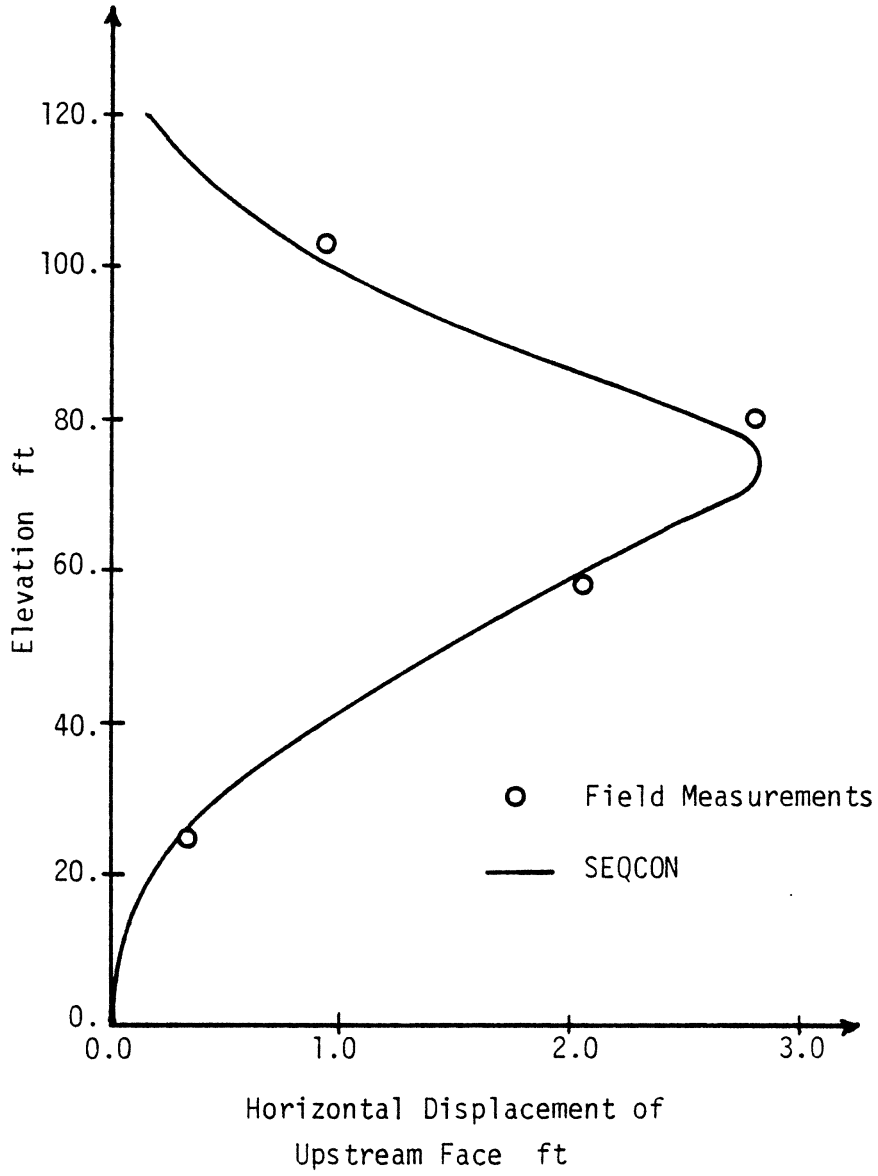


Figure 30: Displacement of Otter Brook Dam Face

Modulus Number = 720.0
 Modulus exponent = 0.50
 Failure ratio = 0.8
 Poisson's ratio = 0.30
 $K_o = 0.43$

The mesh, shown in Figure 31, contains 15 elements and 62 nodes. The wall and its movement was modeled by displacing the nodes on line AB to the right in increments. Twenty displacement increments with no iterations were used.

The wall movement was nondimensionalized by dividing by the wall height. The soil resistance was characterized through the use of the classical passive earth pressure coefficient defined as:

$$K_p = \frac{2P}{\gamma H^2} \quad \text{Eq. 6.4}$$

Where

K_p = Passive earth pressure coefficient

P = Total wall pressure

γ = Unit weight of soil

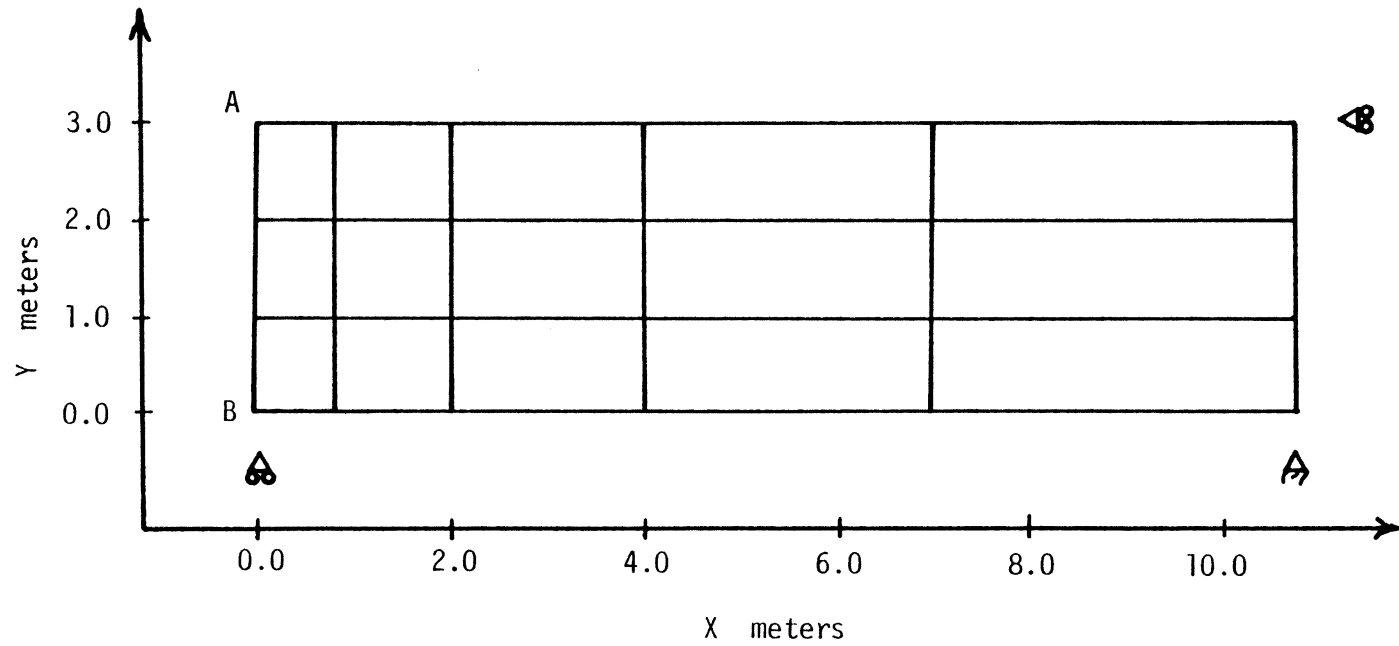


Figure 31: Mesh for Passive Earth Pressure Test

H = Wall height

Figure 32 compares the results obtained from SEQCON and those given by Matsuzaki. The results compare fairly well. Part of the difference between the results may be due to the large number of increments used for the SEQCON calculations. The shape of the curves are quite similar and for large wall displacements both solutions appear to converge to the same answer.

6.6 COMMENTS

The validity of SEQCON as applied to the problems above has been shown. The results, in general, were reasonably accurate. Also, the code was shown to be capable of a wide variety of sequential construction problems.

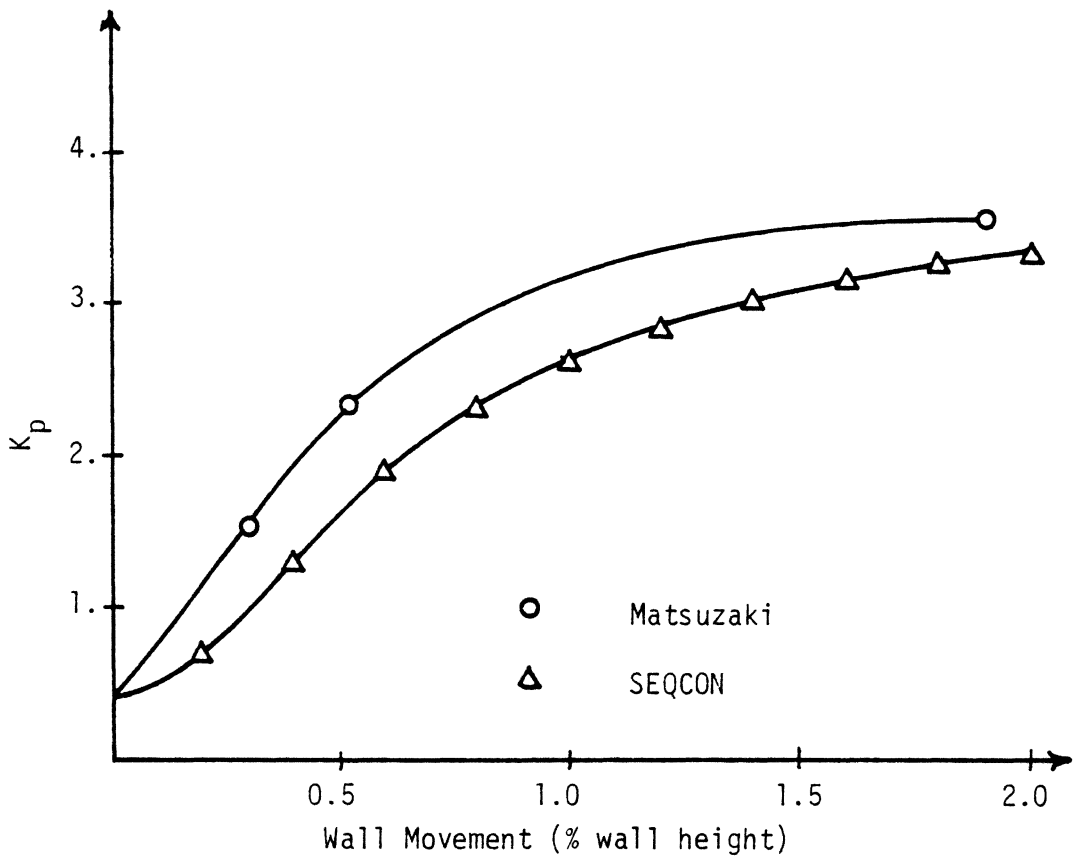


Figure 32: Results for Passive Earth Resistance Test

Chapter VII

CONCLUSIONS

7.1 SUMMARY

A formulation for modeling soil-structure interaction has been presented. In conjunction with the formulation, a computer code was written to implement it. Several problems were analyzed to demonstrate the accuracy of the code.

The program called SEQCON utilizes an eight-node isoparametric quadrilateral. An interface and bar element are also available. Four material models are used. They are the linear elastic, the hyperbolic, the Drucker-Prager, and the cap model.

Several construction sequence steps were modeled. They include in situ, dewatering, excavation, deposition (embankment) and tie-backs. The code itself is modular in design and quite flexible. It is easy to implement and to modify.

The use of SEQCON on various problems has pointed out some of the difficulties of modeling soil-structure interaction problems. The modeling of the interface

behavior is the worst problem. The interface element in SEQCON must be used with caution if accurate results are to be obtained. The material behavior is another difficult problem. The hyperbolic model must be used with caution especially for the stress paths that occur during excavation. The cap model has not been verified for general problems and its use is of a research nature at this time.

7.2 FUTURE RECOMMENDATIONS

A large amount of research in this area remains. Several changes to SEQCON could result in a much more accurate model. These include development of new constitutive models and new interface elements.

A program of laboratory retaining wall model studies in conjunction with numerical studies using SEQCON would also be desirable. This would allow the program to be more thoroughly tested. Such a model has been constructed and will be utilized at later stages in conjunction with improved FE procedures based on mixed and hybrid approaches.

REFERENCES

1. Andrawes, Kamal Z., and El-Sohby, Mohamed A., "Factors Affecting Coefficient for Earth Pressure," Journal of the Soil Mechanics and Foundations Division, ASCE, Vol. 99, No. SM7, Proc. Paper 9863, July, 1973, pp.527-539.
2. Bathe, Klaus-Jurgen and Wilson, Edward L., Numerical Methods in Finite Element Analysis, Prentice-Hall, Inc., Englewood Cliffs, New Jersey, 1976.
3. Brown, C.B. and King, I.P., "Automatic Embankment Analysis: Equilibrium and Instability conditions," Geotechnique, Vol. XVI, No. 3, Sept. 1966, pp. 209-219.
4. Chang, Chin-Yung and Duncan, James M., "Analysis of Soil Movement Around A Deep Excavation," Journal of the Soil Mechanics and Foundations Division, ASCE, Vol. 96, No. SM5, Sept., 1970, pp. 1655-1681.
5. Christian and Desai, "Constitutive Laws for Geologic Media," Numerical Methods in Geotechnical Engineering, Desai and Christian Ed., McGraw Hill Book Company, New York, New York, 1977, pp. 65-115
6. Christian, John T., and Wong, Ing Hieng, "Errors in Simulating Excavations in Elastic Media by Finite Elements," Soils and Foundations, Japanese Society of Soil Mechanics and Foundation Engineering, Vol. 13, No. 1, Mar. 1973, pp. 1-10.
7. Clough, G.W., "Application of the Finite Element Method to Earth-Structure Interaction," Applications of the Finite Element Method in Geotechnical Engineering, Proceedings of the Symposium Held at Vicksburg, Mississippi, May 1972, pp. 1057-1116.
8. Clough, Wayne G. and Duncan, James W., "Finite Element Analysis of Retaining Wall Behavior," Journal of the Soil Mechanics and Foundations Division, ASCE, Vol. 97, No. SM12, Dec. 1971, pp. 1657-1673.

9. Clough, G.W. and Duncan, J.W., Finite Element Analyses of Port Allen and Old River Locks, Report No. TE 69-3 to U.S. Army Engineers Waterways Experiment Station, Sept. 1969.
10. Clough, G. Wayne and Mana, Abdulaziz, I., "Lessons Learned in Finite Element Analyses of Temporary Excavations in Soft Clay," International Conference on Numerical Methods in Geomechanics, 2d, Virginia Polytechnic Institute and State University, 1976.
11. Clough and Tsui, "Static Analysis of Earth Retaining Structures," Numerical Methods in Geotechnical Engineering, Desai and Christian Ed., McGraw Hill Book Company, New York, New York, 1977, pp. 506-527.
12. Clough, G. Wayne and Tsui, Yvet, "Performance of Tied-Back Walls in Clay," Journal of the Geotechnical Engineering Division, ASCE, Vol. 100, No. GT12, Dec. 1974, pp. 1259-1273.
13. Clough, G.W., Weber, P.R., and Lamont, J., "Design and Observation of a Tied-Back Wall," Performance of Earth and Earth-Supported Structures, Vol. I, Part 2, Proceedings, Purdue University, Lafayette, Indiana, June 11-14, 1972, pp. 1367-1389.
14. Clough, Ray W. and Woodward, Richard, J. III, "Analysis of Embankment Stresses and Deformations," Journal of the Soil Mechanics and Foundations Division, ASCE, Vol. 93, No. SM4, July 1967, pp. 529-549.
15. Desai, Chandrakant S., "Numerical Design-Analysis for Piles in Sands," Journal of the Geotechnical Engineering Division, ASCE, Vol. 100, No. GT6, June, 1974, pp. 613-635.
16. Desai, Chandrakant S., "Nonlinear Analyses Using Spline Functions," Journal of the Soil Mechanics and Foundations Division, ASCE, Vol. 97, No. SM10, October, 1971, pp. 1461-1480.
17. Desai, C.S., Elementary Finite Element Method, Prentice Hall, Inc., Englewood Cliffs, New Jersey 07632, 1979.

18. Desai, C.S., Soil-Structure Interaction and Simulation Problems, A Theme Paper, proceedings, International Symposium on Numerical Methods in Soil Mechanics and Rock Mechanics, University of Karlsruhe, West Germany, Sept., 1975.
19. Desai and Abel, Introduction to the Finite Element Method, Van Nostrand Reinhold Company, New York, New York, 1972.
20. Desai, C.S. and Christian, J.T., ed., Numerical Methods in Geotechnical Engineering, McGraw-Hill Book Company, New York, 1977.
21. Desai, C.S., Johnson, Lawrence D., and Hargett, Charles M., "Analysis of Pile-Supported Gravity Lock," Journal of the Geotechnical Engineering Division, ASCE, Vol. 100, No. GT9, Sept., 1974, pp. 1009-1029.
22. Desai, C.S. and Phan, H.V., "Three Dimensional Finite Element Analysis Including Material and Geometric Nonlinearities," Proceedings, Second International Conference on Computational Methods in Nonlinear Mechanics, University of Texas, Austin, Texas, March, 1979.
23. Drucker, D.C., and Prager, W., "Soil Mechanics and Plastic Analysis of Limit Design," Quarterly Applied Mathematics, Vol. 10, No. 2, pp. 157-165, 1952.
24. Duncan, James M. and Chang, Chin-Yung, "Nonlinear Analysis of Stress and Strain in Soils," Journal of the Soil Mechanics and Foundations Division, ASCE, Vol. 96, No. SM5, Sept., 1970, pp. 1629-1653.
25. Dunlop, Peter, and Duncan, James M., "Development of Failure Arcund Excavated Slopes," Journal of the Soil Mechanics and Foundations Division, ASCE, Vol. 96, No. SM2, March, 1970, pp. 471-493.
26. Ghaboussi, Jamshid, Wilson, Edward L. and Isenberg, Jeremy, "Finite Element for Rock Joints and Interfaces," Journal of the Soil Mechanics and Foundations Division, ASCE, Vol. 99, No. SM10, Oct., 1973, pp. 833-848.
27. Goodman, L.E., and Brown, C.B., "Dead Load Stresses and the Instability of Slopes," Journal of the Soil Mechanics and Foundations Division, ASCE, Vol. 89, No. SM3, May, 1963, pp. 103-134.

28. Goodman, R.E., and Christopher, John, "Finite Element Analysis for Discontinuous Rocks," Numerical Methods in Geotechnical Engineering, Desai and Christian Ed., McGraw Hill Book Company, New York, New York, 1977, pp. 148-175.
29. Goodman, Richard E., Taylor, Robert L. and Brekke, Tor L., "A Model for the Mechanics of Jointed Rock," Journal of the Soil Mechanics and Foundations Division, ASCE, Vol. 94, No. SM5, May, 1968, pp. 637-659.
30. Haliburton, T. Allan, "Numerical Analysis of Flexible Retaining Structures," Journal of the Soil Mechanics and Foundations Division, ASCE, Vol. 94, No. SM6, Nov., 1968, pp. 1233-1251.
31. Hanna, Thomas H. and Kurdi, Ibrahim I., "Studies on Anchored Flexible Retaining Walls in Sand," Journal of the Geotechnical Engineering Division, ASCE, Vol. 100, No. GT10, Oct., 1974, pp. 1107-1122.
32. Herrman, Leonard R., "Finite Element Analysis of Contact Problems," Journal of the Engineering Mechanics Division, ASCE, Vol. 104, No. EM5, Oct., 1978, pp. 1043-1057.
33. Hinton, E. and Owen, R.J., Finite Element Programming, Academic Press, New York, 1977.
34. Hood, P., "Frontal Solution Program for Unsymmetric Matrices," International Journal for Numerical Methods in Engineering, Vol. 10, 1976, pp. 379-399.
35. Irons, Bruce M., "Frontal Solution Program for Finite Element Analysis," International Journal for Numerical Methods in Engineering, Vol. 2, 1970, pp. 5-32.
36. Jones, John S., and Brown, Ralph E., "Temporary Tunnel Support by Artificial Ground Freezing," Journal of the Geotechnical Engineering Division, ASCE, Vol. 104, No. GT10, Oct., 1978, pp. 1257-1276.
37. Katona, M.G., et. al, CANDE- A Modern Approach for the Structural Design and Analysis of Buried Culverts, Report No. FHWA-RD-77-5 to Office of Research, Federal Highway Administration, Washington, D.C., Oct., 1976, pp. 127-160.

38. Kausel, Eduardo, Roesset, Jose M., and Christian, John T., "Nonlinear Behavior in Soil-Structure Interaction," Journal of the Geotechnical Engineering Division, ASCE, Vol. 102, No. GT11, Nov., 1976, pp. 1159-1170.
39. Kay, J.N., and Qamar, Mohamed Iqbal, "Evaluation of Tie-Back Anchor Response," Journal of the Geotechnical Engineering Division, ASCE, Vol. 104, No. GT1, Jan., 1978, pp. 7-89.
40. Kulhawy, F., "Embankments and Excavations," Numerical Methods in Geotechnical Engineering, Desai and Christian Ed., McGraw Hill Book Company, New York, New York, 1977, pp. 528-555.
41. Kulhawy, Fred H., and Duncan, James M., "Stresses and Movements in Oroville Dam," Journal of the Soil Mechanics and Foundations Division, ASCE, Vol. 98, No. SM7, July, 1972, pp. 653-665.
42. Kulhawy, F.H., and Duncan, J.M., and Seed, H.B., Finite Element Analysis of Stresses and Movements in Embankments During Construction, Report No. TE 69-4 to U.S. Army Engineers, Waterways Experiment Station, Nov. 1969.
43. Lee, Kenneth I., Adams, Bobby Dean, and Vagneron, Jean-Marie J., "Reinforced Earth Retaining Walls," Journal of the Soil Mechanics and Foundations Division, ASCE, Vol. 99, No. SM10, Oct., 1973, pp. 745-764.
44. Mansur, Charles I., and Alizadeh, M., "Tie-Backs in Clay to Support Sheeted Excavation," Journal of the Soil Mechanics and Foundations Division, ASCE, Vol. 96, No. SM2, March, 1970, pp. 495-509.
45. Massarsch, R., and Broms, Bengt, "Lateral Earth Pressure at Rest in Soft Clay," Journal of the Geotechnical Engineering Division, ASCE, Vol. 102, No. GT10, Oct., 1976, pp. 1041-1047.
46. Matsuzaki, Keiichi, "Prediction of Earth Pressure in Retaining Structure," A Thesis Submitted for the Degree of Doctor of Philosophy, University of New South Wales, Department of Civil Engineering Materials, October, 1978.

47. Moore, John B., Watfiv: Fortran Programming With the Watfiv Compiler, Reston Publishing Company, Inc., Reston, Virginia, 1975.
48. Oden, J.T., and Reddy, J.N., An Introduction to the Mathematical Theory of Finite Elements, John Wiley and Sons, New York, 1976.
49. Osaimi, Ayed E., and Clough, Wayne G., "Fore-Pressure Dissipation During Excavation," Journal of the Geotechnical Engineering Division, ASCE, Vol. 05, No. GT4, April, 1979, pp. 481-498.
50. Popov, E.P., Mechanics of Materials, Prentice Hall, Inc., Englewood Cliffs, N.J., 1952.
51. Prevost, Jean H., "Plasticity Theory for Soil Stress-Strain Behavior," Journal of the Engineering Mechanics Division, ASCE, Vol. 104, No. EM5, Oct., 1978, pp. 1177-1194.
52. Sandler, I.S. and Rubin, D., "An Algorithm and a Modular Subroutine for the Cap Model," International Journal for Numerical and Analytical Methods in Geomechanics, Vol. 3, 1979, pp. 173-186.
53. Sanger, Frederick J., "Ground Freezing in Construction," Journal of the Soil Mechanics and Foundations Division, ASCE, Vol. 94, No. SM1, Jan., 1968, pp. 131-158.
54. Stricklin, J.A., et. al, "On Isoparametric vs. Linear Strain Triangular Elements," International Journal for Numerical Methods in Engineering, Vol. II, No. 6, 1977, pp. 1041-1043.
55. Taylor, David W., "More on Distorted Isoparametric Elements," International Journal for Numerical Methods in Engineering, Vol. 14, No. 2, 1979, pp. 290-291.
56. Tsui, Yvet, and Clough, G. Wayne, "Plane Strain Approximations in Finite Element Analyses of Temporary Walls," Conference on Analysis and Design in Geotechnical Engineering, ASCE, Austin, Texas, 1974, pp. 173-198.
57. Zienkiewicz, O.C., The Finite Element Method, McGraw-Hill Book Company Ltd., London, England, 1977.

58. Zienkiewicz, O.C., et. al., "Analysis of Nonlinear Problems in Rock Mechanics with Particular Reference to Jointed Rock Systems," Proceeding of the 2nd Congress of the International Society for Rock Mechanics, Belgrade, Yugoslavia, 1970.

**The vita has been removed from
the scanned document**

IMPROVED NUMERICAL PROCEDURES FOR SOIL-STRUCTURE INTERACTION
INCLUDING SIMULATION OF CONSTRUCTION SEQUENCES

by

John Gwin Lightner, III

(ABSTRACT)

A formulation for modeling soil-structure interaction has been presented. In conjunction with the formulation, a computer code was written to implement it. Several problems were analyzed to demonstrate the accuracy of the code.

The program called SEQCON utilizes an eight-node isoparametric quadrilateral. An interface and bar element are also available. Four material models are used. They are the linear elastic, the hyperbolic, the Drucker-Prager, and the cap model.

Several construction sequence steps were modeled. They include in situ, dewatering, excavation, deposition (embankment) and tie-backs. The code itself is modular in design and quite flexible. It is easy to implement and to modify.